

Cavity QED materials: Comparison and validation of two linear response theories at arbitrary light-matter coupling strengths

Juan Román-Roche,^{1,2} Álvaro Gómez-León,³ Fernando Luis,^{1,2} and David Zueco^{1,2}

¹*Instituto de Nanociencia y Materiales de Aragón (INMA),
CSIC-Universidad de Zaragoza, Zaragoza 50009, Spain*

²*Departamento de Física de la Materia Condensada,
Universidad de Zaragoza, Zaragoza 50009, Spain*

³*Institute of Fundamental Physics IFF-CSIC, Calle Serrano 113b, 28006 Madrid, Spain*

(Dated: June 19, 2024)

We develop a linear response theory for materials collectively coupled to a cavity that is valid in all regimes of light-matter coupling, including symmetry-broken phases. We present and compare two different approaches. First, using a coherent path integral formulation for the partition function to obtain thermal Green functions. This approach relies on a saddle point expansion for the action, that can be truncated in the thermodynamic limit. Second, by formulating the equations of motion for the retarded Green functions and solving them. We use a mean-field decoupling of high-order Green functions in order to obtain a closed, solvable system of equations. Both approaches yield identical results in the calculation of response functions for the cavity and material. These are obtained in terms of the bare cavity and material responses. In combination, the two techniques clarify the validity of a mean-field decoupling in correlated light-matter systems and provide complementary means to compute finite-size corrections to the thermodynamic limit. The theory is formulated for a general model that encompasses most of the systems typically considered in the field of cavity QED materials, within a long-wavelength approximation. Finally, we provide a detailed application of the theory to the Quantum Hall effect and to a collection of magnetic models. We validate our predictions against analytical and finite-size exact-diagonalization results.

I. INTRODUCTION

Linear Response Theory (LRT) is an elegant tool for understanding how systems at equilibrium respond when they are perturbed. The linearity refers to the condition that the perturbation is sufficiently weak, allowing the system's dynamics to be treated to first order in the perturbation. This framework yields various relations that determine response properties, regardless of the specific situation or model considered. Fundamentally, it relates equilibrium fluctuations and dissipation through the fluctuation-dissipation theorem [1][Chap. 7].

In this paper, we investigate a particular scenario where a system containing N local degrees of freedom is coupled to a single-mode cavity. The coupling is assumed to be collective, and our theory yields exact results in the thermodynamic limit for the matter, $N \rightarrow \infty$. This is the typical limit considered in cavity QED materials, on which we will elaborate below [2–4]. Beyond the assumption of collective coupling and the thermodynamic limit, our approach is general. We obtain formulas for the response of both the material and the cavity in terms of the bare photonic and material response functions, for any light-matter coupling strength. At equilibrium, it has been shown that the $N \rightarrow \infty$ limit simplifies the problem, allowing for exact results, particularly famous is the existence (or lack thereof) of the superradiant phase transition. Various techniques have been employed, including thermodynamic inequalities [5], scaling arguments [6], the stiffness theorem [7], and path integral methods [8]. In this work, we are interested in perturbing the equilibrium to build an equally rigorous result

for LRT. To achieve this, we use two independent but complementary approaches: one based on a path integral formulation of the partition function and the other on the equations of motion for the correlators. The main idea underpinning our derivation is the fact that collective interactions can be exactly decoupled by an auxiliary mean-field variable. This is a common resource in large- N theories in quantum field theory which is used in combination with a saddle-point approximation for the action [9]. The complementary formulation in terms of the equations of motion for the correlators renounces the provable exactness afforded by the path integral in exchange for a simpler derivation where the mean-field decoupling is explicit.

Cavity QED materials are actively discussed in the literature, particularly the possibility of modifying the properties of matter using quantum light [2, 3]. This is pertinent in the regime of strong light-matter correlations, which is why a non-perturbative approach is relevant. The problem is far from being a theoretical curiosity, as initial experiments have reported modifications in conductivity [10, 11], magnetism [12], and metal-to-insulator transition [13]. Remarkably, one way to observe these modifications is through the hybrid light-matter response, which is where our work fits, providing a general theory for such situations. In this context, our work presents the LRT for cavity materials using both a path-integral and an equations-of-motion approach. We discuss their relationship and the application of our theory. We demonstrate that our theory recovers previous results on the cavity-modified quantum Hall effect and explore the response of magnetic materials in cavities,

discussing dipolar Ising systems with longitudinal and transverse coupling to the cavity, Heisenberg ferromagnetism, and the Dicke-Ising model. The latter involves a one-dimensional Ising chain coupled to a cavity, allowing for finite-size numerical simulations to validate our general theory. It should be noted that this paper is quite technical and is accompanied by a letter focusing on the presentation of the main formulas and their use [14]. In the letter, we also discuss the emergence of a new type of bound polariton state in the Dicke-Ising model. Here, we delve into all the theoretical details and provide the aforementioned examples not fully covered in the letter.

The paper is organized as follows. In Sec. II we present the Hamiltonian and discuss its validity to describe the typical models of cavity QED materials. In Sec. III we develop and compare two distinct linear response theories. We provide expressions for different response functions of the hybrid light-matter system in terms of the bare response functions of the cavity and the material. Section IV is dedicated to the application of the LRT to the quantum Hall effect. More precisely to a 2D electron gas subject a homogeneous perpendicular classical magnetic field. In Sec. V we apply the theory to several magnetic models: the Dicke model, the LMG model with longitudinal coupling to a cavity, the Dicke-LMG model, the Dicke-Ising model and the Heisenberg model. We end the paper with some Conclusions and relegate some technical details to the Appendices.

II. MODELS IN CAVITY QED MATERIALS

We will consider a Hamiltonian of the form

$$H = H_m + \Omega a^\dagger a + g(a + a^\dagger) C_x + \zeta \frac{g^2}{\Omega} C_x^2. \quad (1)$$

Here the bare material system is described by H_m and remains unspecified. Likewise C_x is an unspecified Hermitian matter coupling operator. The light matter coupling constant $g = \lambda/\sqrt{N}$ represents the coupling per particle, with λ the collective coupling. The last term is an optional P^2 term, toggled by $\zeta \in \{0, 1\}$.

Depending on the choice of H_m , C_x , Ω , g and ζ this Hamiltonian can describe several distinct microscopic systems. The Pauli-Fierz Hamiltonian can be brought to the form of Hamiltonian (1) by invoking the long-wavelength approximation and diagonalizing the photonic sector with a Bogoliubov transformation to eliminate the A^2 term [7, 8, 15]. It would correspond to setting $\zeta = 0$ and associating the electronic collective momenta to C_x and renormalized frequency and couplings, stemming from the Bogoliubov transform, to Ω and g (See Sec. IV for an example). Fermi-Hubbard models cannot be cast to the form of Hamiltonian (1) due to the non-linear nature of the Peierls coupling, unless it is linearized by considering the weak coupling limit or by moving to the dipole gauge [16–18]. Localized electric

dipoles can be described by setting $\zeta = 1$ and associating the collective dipole operator to C_x [8, 19]. Since the inclusion of the P^2 term to ensure gauge invariance is a relatively recent mandate and many common models do not incorporate it, toggling off ζ will clarify its effects within linear response theory [20]. Furthermore, we consider ζ a binary parameter here, but promoting it to take arbitrary values also allows to study a model where the P^2 term amplitude is not fixed by the light-matter coupling and cavity frequency. To describe magnetic dipoles instead, one can associate a collective spin operator to C_x and toggle off the P^2 term by setting $\zeta = 1$ [21–23]. Finally, a system of coupled oscillators is also compatible with Hamiltonian (1), although solving it with the theory described in this paper would be overkill.

III. LINEAR RESPONSE THEORY

Throughout this text, we will compute linear response functions, i.e. retarded Green functions, for the light and matter subsystems. In our derivation, we will not specify the matter subsystem; instead, we will derive relationships between the Green functions for the hybrid light-matter system with the bare matter and photonic Green functions. The bare photonic Green function is a well know quantity that is trivial to compute. A full solution will thus be contingent on being able to compute the Green function of the bare matter, possibly subject to some additional mean fields, as we will gather from the derivation. The retarded Green function for operators A and B is defined as

$$G_{A,B}^r(t, t') = -i\theta(t - t')\langle [A(t), B(t')] \rangle. \quad (2)$$

We will be particularly concerned with the photonic propagator

$$D(t) = G_{a,a^\dagger}^r(t, 0) \quad (3)$$

and matter response functions

$$\chi_{ab}(t) = -\frac{1}{N} G_{C_a, C_b}^r(t, 0), \quad (4)$$

where C_a might be C_x or any other collective matter operator.

A. Imaginary-time path integral: Thermal Green function

One way to compute retarded Green functions is to obtain them by analytic continuation from the thermal Green function, which can be computed from an imaginary-time path integral formulation of the partition function of the system. The thermal Green function for operators A and B reads

$$G_{A,B}^t(\tau - \tau') = -\langle \mathcal{T}_\tau A(\tau) B(\tau') \rangle \quad (5)$$

Within the imaginary-time formalism, we will obtain the thermal Green functions in terms of imaginary time, τ , or Matsubara frequencies, ω_m . The retarded Green function is then obtained with the replacement

$$G_{A,B}^r(\omega) = G_{A,B}^t(\omega_m)|_{i\omega_m \rightarrow \omega_+ = \omega + i0^+}, \quad (6)$$

for all positive Matsubara frequencies [1][Chap. 7].

1. Effective action

We formulate the partition function as a path integral over coherent states

$$Z = \oint_{a,\bar{a},c} e^{-S}, \quad (7)$$

with

$$S = S_m + \int_{\tau} \bar{a}(\tau)(\partial_{\tau} - \Omega)a(\tau) + g \int_{\tau} (a(\tau) + \bar{a}(\tau))C_x(\tau) + \zeta \frac{g^2}{\Omega} \int_{\tau} C_x^2(\tau). \quad (8)$$

Here $\oint_{a,\bar{a},c} \equiv \int \mathcal{D}[a, \bar{a}] \mathcal{D}[c]$ is the functional integral over coherent-state paths and $\int_{\tau} \equiv \int_0^{\beta} d\tau$ is the integral over imaginary time. A partial integration over the photonic fields, which is but a collection of Gaussian integrals, yields an effective action $S_{\text{eff}} = S_m + S_{\text{ind}}$ with an induced retarded collective interaction [24, 25]

$$S_{\text{ind}} = g^2 \int_{\tau, \tau'} C_x(\tau) D_0(\tau - \tau') C_x(\tau') + \zeta \frac{g^2}{\Omega} \int_{\tau} C_x^2(\tau). \quad (9)$$

Here D_0 is the free photon propagator

$$D_0(\tau) = -\frac{e^{-\tau\Omega}}{1 - e^{-\beta\Omega}}, \quad (10)$$

or in Matsubara frequency space

$$D_0(\omega_m) = \frac{1}{i\omega_m - \Omega}. \quad (11)$$

It is convenient to write

$$S_{\text{ind}} = \frac{1}{2} \int_{\tau, \tau'} C_x(\tau) \frac{1}{N} V_{\text{ind}}(\tau - \tau') C_x(\tau'), \quad (12)$$

with

$$V_{\text{ind}}(\tau) = \lambda^2(D_0(\tau) + D_0(\beta - \tau)) + 2\zeta \frac{\lambda^2}{\Omega} \delta(\tau), \quad (13)$$

or in Matsubara frequency space

$$V_{\text{ind}}(\omega_m) = 2\lambda^2 \frac{\Omega^2(\zeta - 1) + \zeta\omega_m^2}{\Omega(\omega_m^2 + \Omega^2)}. \quad (14)$$

Note that we symmetrize V_{ind} with respect to τ . It can be seen that the odd part of V_{ind} does not contribute to the action. This will be justified later, when we relate V_{ind} to the propagator of an auxiliary real scalar field, which must be even.

2. Auxiliary field decoupling

The induced interaction can be decoupled with a Hubbard-Stratonovich transformation that introduces an auxiliary scalar field, φ :

$$e^{-S_{\text{ind}}} = \frac{1}{Z_{\varphi}} \oint_{\varphi} \exp\left(-\frac{1}{2}N \int_{\tau, \tau'} \varphi(\tau) V_{\text{ind}}^{-1}(\tau - \tau') \varphi(\tau') - i \int_{\tau} \varphi(\tau) C_x(\tau)\right). \quad (15)$$

We define the propagator of the auxiliary field as

$$W(\tau) = \langle \varphi(\tau) \varphi(0) \rangle^c. \quad (16)$$

The generating functional for bare connected correlation functions of the matter coupling operator, C_x , is $\mathcal{G}_m^0[\xi] = -N^{-1} \log Z_m[\xi]$ with

$$Z_m[\xi] = \oint_c e^{-(S_m + i \int_{\tau} \xi(\tau) C_x(\tau))}, \quad (17)$$

such that

$$\begin{aligned} \frac{\delta}{\delta \xi(\tau_1)} \cdots \frac{\delta}{\delta \xi(\tau_n)} \mathcal{G}_m^0[\xi] \Big|_{\xi=0} &= \\ &= -\frac{(-i)^n}{N} \langle C_x(\tau_1) \cdots C_x(\tau_n) \rangle_m^c \\ &\equiv \chi_{xx,0}^{(n)}(\tau_1, \dots, \tau_n). \end{aligned} \quad (18)$$

In the following we will denote $\chi_{xx,0}^{(2)} \equiv \chi_{xx,0}$. With this, after partial integration over the matter degrees of freedom, we can write [26]

$$Z = \oint_{\varphi} e^{-Nf[\varphi]}, \quad (19)$$

with

$$f[\varphi] = \frac{1}{2} \int_{\tau, \tau'} \varphi(\tau) V_{\text{ind}}^{-1}(\tau - \tau') \varphi(\tau') + \mathcal{G}_m^0[\varphi]. \quad (20)$$

The exponent is proportional to N , suggesting that it can be treated with the saddle-point method for large N . The number of terms required for a good approximation will be determined by the value of N . In the thermodynamic limit, $N \rightarrow \infty$, it will be justified to truncate the expansion at the quadratic term, which will reveal what is the free propagator of the auxiliary field φ . The condition that the functional derivative of f with respect to φ vanishes

$$\begin{aligned} \int_{\tau'} V_{\text{ind}}^{-1}(\tau - \tau') \varphi_{\text{sp}}(\tau') + \frac{\delta \mathcal{G}_m^0[\varphi_{\text{sp}}]}{\delta \varphi_{\text{sp}}(\tau)} &= \\ \int_{\tau'} V_{\text{ind}}^{-1}(\tau - \tau') \varphi_{\text{sp}}(\tau') + \frac{i}{N} \langle C_x(\tau) \rangle_{\varphi_{\text{sp}}} &= 0 \end{aligned} \quad (21)$$

or in Matsubara frequency space

$$\varphi_{\text{sp}}(\omega_m) = -\frac{i}{N} V_{\text{ind}}(\omega_m) \langle C_x(\omega_m) \rangle_{\varphi_{\text{sp}}} \quad (22)$$

formally defines φ_{sp} . Let us postpone the issue of finding φ_{sp} for now and continue on by expanding f in powers of φ around φ_{sp} . It is convenient to note that, by definition,

$$\mathcal{G}_m^0[\xi] = \sum_{n_{\text{even}}} \frac{1}{n!} \int_{\tau_1, \dots, \tau_n} \xi(\tau_1) \cdots \xi(\tau_n) \chi_{xx,0}^{(n)}(\tau_1, \dots, \tau_n). \quad (23)$$

Odd terms are absent because the model is invariant under a sign flip of C_x . Therefore

$$f[\varphi] - f[\varphi_{\text{sp}}] = \frac{1}{2} \int_{\tau, \tau'} \delta\varphi(\tau) (NW_0)^{-1}(\tau - \tau') \delta\varphi(\tau') + \mathcal{O}(\varphi^4). \quad (24)$$

Here $\delta\varphi = \varphi - \varphi_{\text{sp}}$ and

$$(NW_0)^{-1} = V_{\text{ind}}^{-1} + \tilde{\chi}_{xx,0}, \quad (25)$$

with

$$\begin{aligned} \tilde{\chi}_{xx,0}(\tau, \tau') &= \frac{\delta}{\delta\varphi_{\text{sp}}(\tau)} \frac{\delta}{\delta\varphi_{\text{sp}}(\tau')} \mathcal{G}_m^0[\varphi_{\text{sp}}] \\ &= \frac{1}{N} \langle C_x(\tau) C_x(\tau') \rangle_{\varphi_{\text{sp}}}^c. \end{aligned} \quad (26)$$

Note that if $\varphi_{\text{sp}} = 0$ then $\tilde{\chi}_{xx,0} = \chi_{xx,0}$. At this point we note that W_0 , which is the free propagator of φ , a real scalar field, is a function of V_{ind} . It now clear why we symmetrize V_{ind} , W_0 must be even in time. The importance of Eq. (25) stems from the fact that for $N \rightarrow \infty$ one can safely truncate the saddle-point expansion to second order, which implies that $W = W_0$. We can now obtain relations between the auxiliary field propagator, W , the photonic propagator, D , and matter response functions.

3. Dressed response functions in terms of bare response functions

In the following we will define generating functionals for connected correlators in imaginary time. These differ from the thermal Green function as defined in Eq. (5) in symmetry broken phases when the expectation value of the operator for which one is computing the connected correlator acquires a finite value. However, this difference only affects the zero frequency component of the correlator and is thus unimportant for the analytic continuation to real frequencies.

Let us define the generating functional for photonic connected correlators by introducing a complex field in

Eq. (7): $\mathcal{G}_{\text{ph}}[\eta, \bar{\eta}] = -\log Z[\eta, \bar{\eta}]$, with

$$Z[\eta, \bar{\eta}] = \oint_{a, \bar{a}, c} e^{-(S + \int_{\tau} (a(\tau) \bar{\eta}(\tau) + \bar{a}(\tau) \eta(\tau))}. \quad (27)$$

After partial integration of the cavity fields, this yields

$$Z[\eta, \bar{\eta}] = \oint_c \exp - \left(S_m + \zeta \frac{g^2}{\Omega} \int_{\tau} C_x^2(\tau) + \int_{\tau, \tau'} \bar{m}(\tau) D_0(\tau - \tau') m(\tau) \right), \quad (28)$$

with $m(\tau) = \eta(\tau) + g C_x(\tau)$. With this

$$\begin{aligned} D(\tau - \tau') &= \frac{\delta}{\delta \bar{\eta}(\tau)} \frac{\delta}{\delta \eta(\tau')} \mathcal{G}_{\text{ph}}[\eta, \bar{\eta}] \Big|_{\eta = \bar{\eta} = 0} \\ &= D_0(\tau - \tau') \\ &\quad - \lambda^2 \int_{u, v} D_0(\tau - u) \chi_{xx}(u - v) D_0(v - \tau'), \end{aligned} \quad (29)$$

or in Matsubara frequency space

$$D(\omega_m) = D_0(\omega_m) - \lambda^2 D_0(\omega_m) \chi_{xx}(\omega_m) D_0(\omega_m). \quad (30)$$

Likewise, we can define the generating functional for matter connected correlators. Since we are interested in response functions, i.e. two point-correlators, we can rather generally consider correlations of three distinct matter operators, the matter coupling operator, C_x , and two others, that we label C_y and C_z . Note that x, y and z are simply indices here and they do not necessarily indicate spatial direction. The generating functional is $\mathcal{G}_m[\xi_x, \xi_y, \xi_z] = -N^{-1} \log Z[\xi_x, \xi_y, \xi_z]$, with

$$Z[\xi_x, \xi_y, \xi_z] = \oint_{c, \varphi} e^{-(S_{\text{eff}} + i \int_{\tau} \sum_a \xi_a(\tau) C_a(\tau))}. \quad (31)$$

After partial integration over the cavity fields, this yields

$$Z[\xi_x, \xi_y, \xi_z] = \oint_{\varphi} e^{-N f[\xi_x + \varphi, \xi_y, \xi_z]}, \quad (32)$$

with

$$\begin{aligned} f[\xi_x + \varphi, \xi_y, \xi_z] &= \frac{1}{2} \int_{\tau, \tau'} \varphi(\tau) V_{\text{ind}}^{-1}(\tau - \tau') \varphi(\tau') \\ &\quad + \mathcal{G}_m^0[\xi_x + \varphi, \xi_y, \xi_z], \end{aligned} \quad (33)$$

Here $\mathcal{G}_m^0[\xi_x, \xi_y, \xi_z] = -N^{-1} \log Z_m[\xi_x, \xi_y, \xi_z]$ is the generalization of $\mathcal{G}_m^0[\xi]$ (17), with

$$Z_m[\xi_x, \xi_y, \xi_z] = \oint_c e^{-(S_m + i \int_{\tau} \sum_a \xi_a(\tau) C_a(\tau))}. \quad (34)$$

Then a second-order expansion of $f[\xi_x + \varphi, \xi_y, \xi_z]$ around φ_{sp} yields

$$f[\xi_x + \varphi, \xi_y, \xi_z] - f[\varphi_{\text{sp}}, 0, 0] = \frac{1}{2} \int_{\tau, \tau'} \left(\delta\varphi(\tau)(NW)^{-1}(\tau - \tau')\delta\varphi(\tau') + \sum_{a,b} \xi_a(\tau)\tilde{\chi}_{ab,0}(\tau - \tau')\xi_b(\tau') \right. \\ \left. + \delta\varphi(\tau) \sum_a \tilde{\chi}_{xa,0}(\tau - \tau')\xi_a(\tau') + \sum_a \xi_a(\tau)\tilde{\chi}_{ax,0}(\tau - \tau')\delta\varphi(\tau) \right). \quad (35)$$

The functional integral over the auxiliary-field displacements $\delta\varphi$ is just a Gaussian integral that we can perform, yielding

$$\mathcal{G}_m[\xi_x, \xi_y, \xi_z] = \text{cst.} + \frac{1}{2} \sum_{a,b} \int_{\tau, \tau'} \xi_a(\tau) \left(\tilde{\chi}_{ab,0}(\tau - \tau') - \int_{u,v} \tilde{\chi}_{ax,0}(\tau - u)NW(u - v)\tilde{\chi}_{xb,0}(u - \tau') \right) \xi_b(\tau'). \quad (36)$$

With this

$$\chi_{ab}(\tau - \tau') = \left. \frac{\delta}{\delta\xi_a(\tau)} \frac{\delta}{\delta\xi_b(\tau')} \mathcal{G}_m[\xi_x, \xi_y, \xi_z] \right|_{\xi_a=0 \forall a} = \tilde{\chi}_{ab,0}(\tau - \tau') - \int_{u,v} \tilde{\chi}_{ax,0}(\tau - u)NW(u - v)\tilde{\chi}_{xb,0}(u - \tau'), \quad (37)$$

or in Matsubara frequency space

$$\chi_{ab}(\omega_m) = \tilde{\chi}_{ab,0}(\omega_m) - \chi_{ax,0}(\omega_m)NW(\omega_m)\chi_{xa,0}(\omega_m). \quad (38)$$

Putting together Eqs. (25) and (38) we arrive at the relations

$$\chi_{xa}(\omega_m) = \frac{\tilde{\chi}_{xa,0}(\omega_m)}{1 + V_{\text{ind}}(\omega_m)\tilde{\chi}_{xx,0}(\omega_m)}, \quad (39)$$

$$\chi_{ax}(\omega_m) = \frac{\tilde{\chi}_{ax,0}(\omega_m)}{1 + V_{\text{ind}}(\omega_m)\tilde{\chi}_{xx,0}(\omega_m)}, \quad (40)$$

$$\chi_{ab}|_{a,b \neq x}(\omega_m) = \tilde{\chi}_{ab,0}(\omega_m) - \frac{\tilde{\chi}_{ax,0}(\omega_m)V_{\text{ind}}(\omega_m)\tilde{\chi}_{xb,0}(\omega_m)}{1 + V_{\text{ind}}(\omega_m)\tilde{\chi}_{xx,0}(\omega_m)}, \quad (41)$$

which together with Eq. (30) give us the dependence of the photonic propagator and matter response functions on the bare matter response function and the free photon propagator. Note from Eqs. (A16) and (34) that $\tilde{\chi}_{ab,0}$ is simply the response function of the bare matter subject to an external field φ_{sp} , the saddle point. Equations (39), (39) and (41) exhibit a structure similar to the response functions commonly derived using the random phase approximation, such as those found in [26]. It is important to highlight that these equations remain valid for all parameter ranges and are applicable to both normal and superradiant phases.

4. Computing the saddle point φ_{sp} .

We should now tackle the issue of finding φ_{sp} . Without specifying the matter subsystem it is reasonable to assume a constant solution, i.e. $\varphi_{\text{sp}}(\tau) = \varphi_{\text{sp}} = \varphi_{\text{sp}}(\omega_m = 0)$ (all other frequency components being zero). Then, from Eq. 22 we find

$$\varphi_{\text{sp}} = -\frac{i}{N} V_{\text{ind}}(\omega_m = 0) \langle C_x \rangle_{\varphi_{\text{sp}}}. \quad (42)$$

This tells us that φ_{sp} is self-consistently proportional to $\langle C_x \rangle_{\varphi_{\text{sp}}}$, i.e. to the expectation value of C_x for the bare matter subject to a field $i\varphi_{\text{sp}} = \frac{1}{N} V_{\text{ind}}(\omega_m = 0) \langle C_x \rangle$. This is precisely the self-consistent condition that arises from computing $\langle C_m \rangle$ from the mean-field Hamiltonian

$$H_{\text{eff}}^{\text{MF}} = H_m + \frac{2\lambda^2(\zeta - 1)}{N\Omega} \langle C_x \rangle C_x - \frac{\lambda^2(\zeta - 1)}{N\Omega} \langle C_x \rangle^2. \quad (43)$$

This is the mean-field theory of the effective Hamiltonian that arises from taking the static limit in V_{ind} in the effective action [8], justifying (42). Thus, if we assume φ_{sp} constant, $\tilde{\chi}_{ab,0}$ are just the response functions of the mean field matter Hamiltonian of Eq. (43). Thus, $\tilde{\chi}_{ab,0}$ are obtained as functions of $\langle C_x \rangle$ which can be computed by solving $H_{\text{eff}}^{\text{MF}}$ variationally with respect to $\langle C_x \rangle$. Note that in the absence of symmetry breaking, i.e. when $\langle C_x \rangle = 0$, or if $\zeta = 1$, the effective matter Hamiltonian is just the bare matter Hamiltonian and thus $\tilde{\chi}_{ab,0} = \chi_{ab,0}$ is just the bare matter response.

B. Equations of motion for the retarded Green functions

An alternative way to compute retarded Green functions is by formulating their equations of motion and, under some assumptions, solving them. Defining $G_{A,B}^r(t) \equiv G_{A,B}^r(t, 0)$ we have from Eq. (2) that

$$i\partial_t G_{A,B}^r(t) = \delta(t) \langle [A, B] \rangle - G_{[H,A],B}^r(t) \quad (44)$$

or in frequency space

$$\omega_+ G_{A,B}^r(\omega) = \langle [A, B] \rangle - G_{[H,A],B}^r(\omega), \quad (45)$$

with $\omega_+ = \omega + i0^+$.

1. Solving the equations of motion

Let $\{|\alpha\rangle\}$ be a basis of the Hilbert space of the matter subsystem and let us define the Hubbard operators

$X^{\alpha\beta} = |\alpha\rangle\langle\beta|$. We start by computing the matter correlation function χ_{ab} . Note that

$$\chi_{ab} = -\frac{1}{N}G_{C_a, C_b}^r = -\frac{1}{N}\sum_{\alpha, \beta} C_a^{\alpha\beta} G_{X^{\alpha\beta}, C_b}^r \quad (46)$$

where $C_a^{\alpha\beta} = \langle\alpha|C_a|\beta\rangle$. Then

$$\begin{aligned} \omega_+ G_{X^{\alpha\beta}, C_b}^r(\omega) &= \langle[X^{\alpha\beta}, C_b]\rangle - G_{[H, X^{\alpha\beta}], C_b}^r(\omega) \\ &= -\Gamma_b^{\alpha\beta} - G_{[H_m, X^{\alpha\beta}], C_b}^r(\omega) \\ &\quad - gG_{(a+a^\dagger)[C_x, X^{\alpha\beta}], C_b}^r(\omega) \\ &\quad - \zeta \frac{g^2}{\Omega} G_{[C_x^2, X^{\alpha\beta}], C_b}^r(\omega). \end{aligned} \quad (47)$$

Here $\Gamma_b^{\alpha\beta} = \langle[C_b, X^{\alpha\beta}]\rangle = \sum_\mu (C_b^{\mu\alpha} \langle X^{\mu\beta} \rangle - C_b^{\beta\mu} \langle X^{\alpha\mu} \rangle)$. The last two terms of Eq. (47) correspond to three-point Green functions. One could now write the equations of motion for such three-point Green functions, which would in turn depend on four-point Green functions, and so on and so forth. This infinite hierarchy of n -point correlators involves light-matter interactions, as discussed in the context of lasing physics [27, Chapter 9] or light emission [28]. At some point, the hierarchy needs to be truncated. The crudest approximation is to restrict the theory to two-point Green functions, assuming that $G_{AB,C}^r \approx \langle A \rangle G_{B,C}^r + \langle B \rangle G_{A,C}^r$, which amounts to neglecting correlations of order higher than two for all terms stemming from light-matter interaction. In terms of fluctuations, this means that only linear fluctuations between the two systems are relevant, and that correlated fluctuations are largely suppressed. This approach is reminiscent of RPA or mean-field approximations, which need to be justified. This has indeed been discussed within the Dicke model, where the traditional educated guess that quantum fluctuations vanish in the $N \rightarrow \infty$ limit [27, Chapter 9] [Cf. with the equilibrium argument in [6]] has been rigorously demonstrated recently [29]. In that work, the proof was restricted to the Dicke model and within the Lindblad framework, *i.e.*, adding dissipation in a Markovian manner. This result is relevant to us since LRT falls within the conditions of the theorem demonstrated in that reference, which requires the dynamics to start with an uncorrelated initial condition between light and matter. This can be safely assumed here since the response is independent of the excitation and can be obtained from excitation functions where the initial condition is assumed to be at equilibrium, which

can be well approximated by uncorrelated light-matter states [7, 23]. It is true, however, that in our case we are not considering dissipative Lindblad dynamics and we include potential matter-matter interactions. In any case, we believe that restricting to two-point Green functions can be proven to be exact, as it agrees with the exactness of the saddle-point solution for $N \rightarrow \infty$ discussed in the previous section. Additionally, this section concludes by obtaining the same response functions as within the path integral formalism. This suggests that generalizing Ref. [29] might be possible in a future work. With this,

$$\begin{aligned} \omega_+ G_{X^{\alpha\beta}, C_b}^r(\omega) &= -\Gamma_b^{\alpha\beta} - G_{[H_m, X^{\alpha\beta}], C_b}^r(\omega) \\ &\quad - g\langle a + a^\dagger \rangle G_{[C_x, X^{\alpha\beta}], C_b}^r(\omega) \\ &\quad - \zeta \frac{2g^2}{\Omega} \langle C_x \rangle G_{[C_x, X^{\alpha\beta}], C_b}^r(\omega) \\ &\quad - g\Gamma_x^{\alpha\beta} \left(G_{a, C_b}^r(\omega) + G_{a^\dagger, C_b}^r(\omega) \right) \\ &\quad - \zeta \frac{2g^2}{\Omega} \Gamma_x^{\alpha\beta} G_{C_x, C_b}^r(\omega). \end{aligned} \quad (48)$$

We can put together the second, third and fourth elements in the right-hand side to build a mean field matter Hamiltonian

$$H_m^{\text{MF}} = H_m - g\langle a + a^\dagger \rangle C_x - \zeta \frac{2g^2}{\Omega} \langle C_x \rangle C_x. \quad (49)$$

Note that the constant terms in this mean-field Hamiltonian are omitted here. We will show later that this Hamiltonian is equivalent to the mean-field effective Hamiltonian (43) obtained with the path integral approach under a mean-field decoupling of full light-matter Hamiltonian. At this point we can assume that the basis that we have been using, $\{|\alpha\rangle\}$, is precisely the eigenbasis of H_m^{MF} , with eigenenergies $\{E_\alpha\}$, obtaining

$$\begin{aligned} \omega_+ G_{X^{\alpha\beta}, C_b}^r(\omega) &= -\Gamma_b^{\alpha\beta} - (E_\alpha - E_\beta) G_{X^{\alpha\beta}, C_b}^r(\omega) \\ &\quad - g\Gamma_x^{\alpha\beta} \left(G_{a, C_b}^r(\omega) + G_{a^\dagger, C_b}^r(\omega) \right) \\ &\quad - \zeta \frac{2g^2}{\Omega} \Gamma_x^{\alpha\beta} G_{C_x, C_b}^r(\omega). \end{aligned} \quad (50)$$

We can compute the photon-matter Green functions that appear on the second line obtaining

$$(\omega_+ - \Omega) G_{a, C_b}^r(\omega) = g G_{C_x, C_b}^r(\omega), \quad (51)$$

$$(\omega_+ + \Omega) G_{a^\dagger, C_b}^r(\omega) = -g G_{C_x, C_b}^r(\omega). \quad (52)$$

Putting together Eqs. (50), (51) and (52) we get

$$(\omega_+ + E_\alpha - E_\beta) G_{X^{\alpha\beta}, C_b}^r(\omega) = -\Gamma_b^{\alpha\beta} - \Gamma_x^{\alpha\beta} V_{\text{ind}}(\omega) \frac{1}{N} G_{C_x, C_b}^r(\omega), \quad (53)$$

with $V_{\text{ind}}(\omega) = V_{\text{ind}}(\omega_m)|_{i\omega_m \rightarrow \omega+i0^+}$. Together with Eq. (46) this gives

$$\chi_{ab}(\omega) = \frac{1}{N} \sum_{\alpha\beta} C_a^{\alpha\beta} \frac{\Gamma_b^{\alpha\beta}}{\omega_+ + E_\alpha - E_\beta} - \frac{1}{N} \sum_{\alpha\beta} C_a^{\alpha\beta} \frac{\Gamma_x^{\alpha\beta}}{\omega_+ + E_\alpha - E_\beta} V_{\text{ind}}(\omega) \chi_{xb}(\omega). \quad (54)$$

From the definition of $\Gamma_b^{\alpha\beta}$ and noting that $\langle X^{\alpha\beta} \rangle = Z^{-1} \delta_{\alpha\beta} \exp(-\beta E_\alpha)$ we find that

$$\frac{1}{N} \sum_{\alpha\beta} C_a^{\alpha\beta} \frac{\Gamma_b^{\alpha\beta}}{\omega_+ + E_\alpha - E_\beta} = \frac{1}{N} \frac{1}{Z} \sum_{\alpha\beta} \frac{e^{-\beta E_\beta} - e^{-\beta E_\alpha}}{\omega_+ + E_\alpha - E_\beta} \langle \alpha | C_a | \beta \rangle \langle \beta | C_b | \alpha \rangle = \tilde{\chi}_{ab,0}(\omega). \quad (55)$$

Note here the abuse of notation by using β both as an index and as inverse temperature. With this and Eq. (54), we finally obtain

$$\chi_{xa}(\omega) = \frac{\tilde{\chi}_{xa,0}(\omega)}{1 + V_{\text{ind}}(\omega) \tilde{\chi}_{xx,0}(\omega)}, \quad (56)$$

$$\chi_{ax}(\omega) = \frac{\tilde{\chi}_{ax,0}(\omega)}{1 + V_{\text{ind}}(\omega) \tilde{\chi}_{xx,0}(\omega)}, \quad (57)$$

$$\chi_{aa|_{a,b \neq x}}(\omega) = \tilde{\chi}_{ab,0}(\omega) - \frac{\tilde{\chi}_{ax,0}(\omega) V_{\text{ind}}(\omega) \tilde{\chi}_{xb,0}(\omega)}{1 + V_{\text{ind}}(\omega) \tilde{\chi}_{xx,0}(\omega)}, \quad (58)$$

which coincide with the analytic continuation of Eqs. (39), (40) and (41).

Proceeding in a similar fashion, we can now compute D and $D_+ = G_{a^\dagger, a^\dagger}^r$. First we have

$$(\omega_+ - \Omega)D(\omega) = 1 + gG_{C_x, a^\dagger}^r(\omega), \quad (59)$$

$$(\omega_+ + \Omega)D_+(\omega) = -gG_{C_x, a^\dagger}^r(\omega). \quad (60)$$

Again we use the decomposition $G_{C_x, a^\dagger}^r = \sum_{\alpha\beta} C_x^{\alpha\beta} G_{X^{\alpha\beta}, a^\dagger}^r$ and compute

$$\begin{aligned} (\omega_+ + E_\alpha - E_\beta)G_{X^{\alpha\beta}, a^\dagger}^r &= -g\Gamma_b^{\alpha\beta} (D(\omega) + D_+(\omega)) \\ &\quad - \zeta \frac{2g^2}{\Omega} \Gamma_b^{\alpha\beta} G_{C_x, a^\dagger}^r(\omega), \end{aligned} \quad (61)$$

such that

$$G_{C_x, a^\dagger}^r = \frac{-Ng\tilde{\chi}_{xx,0}(\omega)}{1 + \zeta \frac{2\lambda^2}{\Omega} \tilde{\chi}_{xx,0}(\omega)} (D(\omega) + D_+(\omega)). \quad (62)$$

Plugging this into Eqs. (59) and (60) we get

$$\begin{aligned} (\omega - \Omega)D(\omega) &= 1 \\ &\quad - \frac{\lambda^2 \tilde{\chi}_{xx,0}(\omega)}{1 + \zeta \frac{2\lambda^2}{\Omega} \tilde{\chi}_{xx,0}(\omega)} (D(\omega) + D_+(\omega)), \end{aligned} \quad (63)$$

$$(\omega + \Omega)D_+(\omega) = \frac{\lambda^2 \tilde{\chi}_{xx,0}(\omega)}{1 + \zeta \frac{2\lambda^2}{\Omega} \tilde{\chi}_{xx,0}(\omega)} (D(\omega) + D_+(\omega)). \quad (64)$$

We can now solve for D and D_+ to get

$$D(\omega) = \frac{\omega_+ + \Omega + \lambda^2 \frac{2\zeta(\omega_+ + \Omega) - \Omega}{\Omega} \tilde{\chi}_{xx,0}(\omega)}{\omega_+^2 - \Omega^2 + 2\lambda^2 \frac{\zeta(\omega_+^2 - \Omega^2) + \Omega^2}{\Omega} \tilde{\chi}_{xx,0}(\omega)}, \quad (65)$$

$$D_+(\omega) = \frac{\lambda^2 \tilde{\chi}_{xx,0}(\omega)}{\omega_+^2 - \Omega^2 + 2\lambda^2 \frac{\zeta(\omega_+^2 - \Omega^2) + \Omega^2}{\Omega} \tilde{\chi}_{xx,0}(\omega)}. \quad (66)$$

Although not immediately obvious, Eq. (65) is precisely the analytic continuation of Eq. (30).

2. Mean field decoupling of the light-matter Hamiltonian

Let us consider the Hamiltonian in Eq. (1) with a mean-field decoupling of the light-matter interaction and P^2 terms. We expand $C_x = \langle C_x \rangle + \delta C_x$ and $a + a^\dagger = \langle a + a^\dagger \rangle + \delta(a + a^\dagger)$ and neglect terms quadratic in fluctuations, obtaining two decoupled Hamiltonians and some constants: $H = H_m^{\text{MF}} + H_{\text{ph}}^{\text{MF}} + \text{cst.}$ with

$$H_m^{\text{MF}} = H_m + g\langle a + a^\dagger \rangle C_x - \zeta \frac{2g^2}{\Omega} \langle C_x \rangle C_x, \quad (67)$$

$$H_{\text{ph}}^{\text{MF}} = \Omega a^\dagger a + g(a + a^\dagger) \langle C_x \rangle, \quad (68)$$

$$\text{cst.} = -g\langle a + a^\dagger \rangle \langle C_x \rangle - \zeta \frac{2g^2}{\Omega} \langle C_x \rangle^2. \quad (69)$$

The mean-field photonic Hamiltonian $H_{\text{ph}}^{\text{MF}}$ can be diagonalized with a displacement, $a = b - g/\Omega \langle C_x \rangle$, yielding $H_{\text{ph}}^{\text{MF}} = \Omega b^\dagger b$, a new constant $-g^2/\Omega \langle C_x \rangle^2$ and the relation $\langle a + a^\dagger \rangle = -2g/\Omega \langle C_x \rangle$. Plucking this relation into the mean-field matter Hamiltonian, H_m^{MF} , and all the constants gathered in the different steps yields precisely the mean-field effective Hamiltonian, $H_{\text{eff}}^{\text{MF}}$, of Eq. (43). The constants are important for a potential variational solution.

C. Comparing the two theories

In this section we have shown the equivalence between two different approaches to address the linear response regime of cavity QED materials. Although seemingly very different, the path-integral in imaginary time and

the equation of motion in real time provide exact analytical results in the thermodynamic limit, $N \rightarrow \infty$. The effect of the thermodynamic limit is clearly identified in the path integral approach when the saddle point method is invoked. Instead, with the equation of motion method it requires an analysis of the scaling of the correlated parts of higher-order correlation functions with N . On the other hand, the equations-of-motion approach does not require the auxiliary field of the Hubbard-Stratonovich transformation, which allows us to interpret the steps used to calculate its propagator W . We can see that the auxiliary field φ_{sp} plays the same role as the mean-field background in the equation of motion, which couples to the fluctuations. Together, the two approaches cement the understanding that mean-field approaches are exact in the thermodynamic limit for Dicke-like models, even if matter interactions are considered. This has been studied and exploited before at equilibrium [6–8, 23, 30] and in the dynamics [29] and in Refs. [26, 31] and now here for the LRT. Beyond the LRT, the equations-of-motion approach opens the possibility of studying real-time dynamics.

Finally, the comparison between the two approaches is not just an academic exercise. In many cases it can be interesting to go beyond the $N \rightarrow \infty$ limit. This would be the case in topological systems, where boundaries play an important role. In that case the two approaches offer complementary methods incorporate finite-size corrections. In the path integral approach, corrections are computed by extending the saddle-point expansion to higher orders, and thus relaxing $W = W_0$ for the weaker $W^{-1} = W_0^{-1} + \Pi$, where Π can be computed with standard diagrammatic techniques in terms of fourth- and higher-order matter response functions [26]. In the equations-of-motion approach, corrections are introduced by expanding the theory from two- to three- and higher-order Green functions before invoking the mean-field factoring of the correlators.

IV. INTEGER QUANTUM HALL EFFECT IN A CAVITY

A. The Hamiltonian

To demonstrate the applicability of our theory, we will use it to study the modification of the integer quantum Hall effect. The matter system under consideration is a two-dimensional electron gas subject to a perpendicular classical magnetic field. This model has been used to explain the breakdown of topological protection that underlies the observed modifications of the quantum Hall effect by coupling to a cavity [11, 32–34]. The Hamiltonian of the electron gas coupled to a single-mode cavity

reads

$$H = \sum_j \frac{(\mathbf{p}_j - e\mathbf{A}_{\text{ext}}(\mathbf{r}_j) - e\mathbf{A}_0(b + b^\dagger))^2}{2m} + \sum_{i>j} V(\mathbf{r}_i - \mathbf{r}_j) + \Omega b^\dagger b. \quad (70)$$

Here \mathbf{r}_i , \mathbf{p}_i are respectively the position and momentum operators of the i -th electron. Both the external classical vector potential and the cavity's vector potential point along the x -direction: $\mathbf{A}_{\text{ext}}(\mathbf{r}_j) = -By_j\mathbf{e}_x$ and $\mathbf{A}_0 = \sqrt{1/(2\epsilon_0 V \Omega)}\mathbf{e}_x$. The V and ϵ_0 are respectively the cavity mode volume and the dielectric constant. $V(\mathbf{r}_i - \mathbf{r}_j)$ is the Coulomb interaction between the electrons. After some manipulation, we can write the Hamiltonian as

$$H = H_m - \frac{\omega_p}{\sqrt{N}} \left(\sqrt{\frac{\omega_p}{\Omega}} \bar{p}_x + \sqrt{\frac{\omega_c}{\Omega}} \bar{y} \right) (b + b^\dagger) + \Omega b^\dagger b + \frac{\omega_p^2}{4\Omega} (b + b^\dagger)^2, \quad (71)$$

where H_m is the bare (without cavity) electron gas Hamiltonian

$$H_m = \sum_j \frac{(\mathbf{p}_j - e\mathbf{A}_{\text{ext}}(\mathbf{r}_j))^2}{2m} + \sum_{i>j} V(\mathbf{r}_i - \mathbf{r}_j) \quad (72)$$

and \bar{p}_x and \bar{y} are adimensionalized collective operators

$$\bar{p}_x = \frac{1}{\sqrt{2m\omega_p}} \sum_j p_{x,j}, \quad (73)$$

$$\bar{y} = \sqrt{\frac{m\omega_c}{2}} \sum_j y_j. \quad (74)$$

We have defined the plasma frequency, $\omega_p = \sqrt{e^2\rho/(m\epsilon_0)}$ with $\rho = N/V$ the density of electrons in the cavity, and the cyclotron frequency $\omega_c = eB/m$. The photonic terms of the Hamiltonian can be diagonalized with a Bogoliubov transformation, which yields

$$H = H_m - \frac{\omega_p}{\sqrt{N}} \left(\sqrt{\frac{\omega_p}{\tilde{\omega}}} \bar{p}_x + \sqrt{\frac{\omega_c}{\tilde{\omega}}} \bar{y} \right) (a + a^\dagger) + \tilde{\omega} a^\dagger a, \quad (75)$$

with $\tilde{\omega}^2 = \Omega^2 + \omega_p^2$. By identifying $g = -\omega_p/\sqrt{N}$ and $C_x = \sqrt{\omega_p/\tilde{\omega}}\bar{p}_x + \sqrt{\omega_c/\tilde{\omega}}\bar{y}$ the Hamiltonian takes the form of Eq. (1). Note that in this case there is no P^2 term, i.e. $\zeta = 0$, as we are working in the Coulomb gauge. In exchange, the elimination of the A^2 term through the Bogoliubov transform renormalizes the cavity frequency and light-matter coupling.

B. Current and optical conductivity

In the quantum Hall effect [35, 36], one is typically interested in computing the longitudinal and transverse

conductivities. The optical conductivity tensor can be computed with the Kubo formalism in terms of the current response functions

$$\sigma_{ab}(\omega) = \frac{i}{\omega_+} \left[\frac{e^2 \rho_{2D}}{m} \delta_{ab} + \frac{G_{J_a, J_b}^r(\omega)}{A} \right], \quad (76)$$

where $\omega_+ = \omega + i\delta$, A and ρ_{2D} are the area and surface density of the two-dimensional electron gas, δ is the broadening parameter, δ_{ab} is the Kronecker delta and $J_{a,b}$ are the current operators in the a and b directions, with $a, b \in \{x, y\}$ [37, 38]. We will now compute G_{J_a, J_b}^r using the theory outlined in Sec. III, i.e. we will express G_{J_a, J_b}^r in terms of the response functions of the bare electron gas, G_{J_a, J_b}^{r0} .

The current operator is given by

$$\begin{aligned} \mathbf{J} &= e \sum_j \mathbf{v}_j \\ &= \frac{e}{m} \sum_j (\mathbf{p}_j - e \mathbf{A}_{\text{ext}}(\mathbf{r}_j) - e \mathbf{A}_0(b + b^\dagger)). \end{aligned} \quad (77)$$

Then, after some manipulation, we can express

$$J_x = \sqrt{\frac{2e^2 \tilde{\omega}}{m}} (C_x + \gamma(a + a^\dagger)), \quad (78)$$

$$J_y = \sqrt{\frac{2e^2 \tilde{\omega}}{m}} C_y, \quad (79)$$

with $\gamma = -\sqrt{N} \omega_p / (2\tilde{\omega})$ and $C_y = \sqrt{\omega_p / \tilde{\omega}} \bar{p}_y$. Here $\sqrt{2m\omega_p} \bar{p}_y = \sum_j p_{y,j}$. Meaning that we need to compute

$$G_{J_x, J_x}^r = \frac{2e^2 \tilde{\omega}}{m} G_{C_x + \gamma(a + a^\dagger), C_x + \gamma(a + a^\dagger)}^r, \quad (80)$$

$$G_{J_x, J_y}^r = \frac{2e^2 \tilde{\omega}}{m} G_{C_x + \gamma(a + a^\dagger), C_y}^r, \quad (81)$$

$$G_{J_y, J_y}^r = \frac{2e^2 \tilde{\omega}}{m} G_{C_y, C_y}^r. \quad (82)$$

C. Implicit expressions for the current response functions

1. Computing mixed light-matter correlations

To compute these alternative Green functions following our section III, we formulate the following generating functional for mixed connected correlators:

$\mathcal{G}_{\text{mix}}[\eta, \xi_x, \xi_y] = -\log Z[\eta, \xi_x, \xi_y]$, with

$$\begin{aligned} Z[\eta, \xi_x, \xi_y] &= \oint_{a, \bar{a}, c} \exp \left(S + \int_\tau \eta(\tau) (a(\tau) + \bar{a}(\tau)) \right. \\ &\quad \left. + \sum_a \int_\tau \xi_a(\tau) C_a(\tau) \right). \end{aligned} \quad (83)$$

After partial integration of the cavity fields, this yields

$$\begin{aligned} Z[\eta, \xi_x, \xi_y] &= \oint_c \exp \left(S_m + \int_{\tau, \tau'} m(\tau) D_0(\tau - \tau') m(\tau) \right. \\ &\quad \left. + \sum_a \int_\tau \xi_a(\tau) C_a(\tau) \right), \end{aligned} \quad (84)$$

with $m(\tau) = \eta(\tau) + g C_x(\tau)$. With this

$$\begin{aligned} G_{\gamma(a+a^\dagger), C_a}^t(\tau - \tau') &= -\gamma \frac{\delta}{\delta \eta(\tau)} \frac{\delta}{\delta \xi_a(\tau')} \mathcal{G}_{\text{mix}}[\eta, \xi_x, \xi_y] \\ &= \gamma \int_u D_0^s(\tau - u) N g \chi_{xa}(u - \tau'), \end{aligned} \quad (85)$$

or in Matsubara frequency space

$$G_{\gamma(a+a^\dagger), C_a}^t(\omega_m) = -\gamma D_0^s(\omega_m) N g \chi_{xa}(\omega_m). \quad (86)$$

Here $D_0^s(\tau) = D_0(\tau) + D_0(-\tau)$ is the symmetrized free photon propagator

$$D_0^s(\omega_m) = \frac{1}{i\omega_m - \tilde{\omega}} - \frac{1}{i\omega_m + \tilde{\omega}}. \quad (87)$$

Likewise

$$G_{C_x, \gamma(a+a^\dagger)}^t(\omega_m) = -\gamma D_0^s(\omega_m) N g \chi_{xx}(\omega_m) \quad (88)$$

and

$$\begin{aligned} G_{\gamma(a+a^\dagger), \gamma(a+a^\dagger)}^t(\omega_m) &= \gamma^2 D_0^s(\omega_m) \\ &\quad - \gamma^2 D_0^s(\omega_m) \lambda^2 \chi_{xx}(\omega_m) D_0^s(\omega_m). \end{aligned} \quad (89)$$

With these we obtain, after analytic continuation $i\omega_m \rightarrow \omega_+$,

$$\begin{aligned} G_{J_x, J_y}^r(\omega) &= -N \frac{2e^2 \tilde{\omega}}{m} (1 + \gamma g D_0^s(\omega)) \chi_{xy}(\omega), \\ &= -N \frac{2e^2 \tilde{\omega}}{m} \left(1 + \left(\frac{\omega_p}{\tilde{\omega}} \right)^2 \frac{\tilde{\omega}}{2} D_0^s(\omega) \right) \chi_{xy}(\omega), \end{aligned} \quad (90)$$

and similarly

$$G_{J_x, J_x}^r(\omega) = -N \frac{2e^2 \tilde{\omega}}{m} \left(\left(1 + \left(\frac{\omega_p}{\tilde{\omega}} \right)^2 \frac{\tilde{\omega}}{2} D_0^s(\omega) \right)^2 \chi_{xx}(\omega) - \frac{1}{2\tilde{\omega}} \left(\frac{\omega_p}{\tilde{\omega}} \right)^2 \frac{\tilde{\omega}}{2} D_0^s(\omega) \right), \quad (91)$$

$$G_{J_y, J_y}^r(\omega) = -N \frac{2e^2 \tilde{\omega}}{m} \chi_{yy}(\omega). \quad (92)$$

We can relate χ_{xx} , χ_{xy} and χ_{yy} to $\tilde{\chi}_{xx,0}$, $\tilde{\chi}_{xy,0}$ and $\tilde{\chi}_{yy,0}$ through Eqs. (39) and (41), obtaining

$$G_{J_x, J_y}^r(\omega) = \left(1 + \left(\frac{\omega_p}{\tilde{\omega}} \right)^2 \frac{\tilde{\omega}}{2} D_0^s(\omega) \right) \frac{\tilde{G}_{J_x, J_y}^{r,0}(\omega)}{1 - V_{\text{ind}}(\omega) \frac{m}{2e^2 \tilde{\omega} N} \tilde{G}_{J_x, J_x}^{r,0}(\omega)}, \quad (93)$$

with $\tilde{G}_{J_a, J_b}^{r,0} = -N \tilde{\chi}_{ab,0}$. Likewise

$$G_{J_x, J_x}^r(\omega) = \left(1 + \left(\frac{\omega_p}{\tilde{\omega}} \right)^2 \frac{\tilde{\omega}}{2} D_0^s(\omega) \right)^2 \frac{\tilde{G}_{J_x, J_x}^{r,0}(\omega)}{1 - V_{\text{ind}}(\omega) \frac{m}{2e^2 \tilde{\omega} N} \tilde{G}_{J_x, J_x}^{r,0}(\omega)} + \frac{Ne^2}{m} \left(\frac{\omega_p}{\tilde{\omega}} \right)^2 \frac{\tilde{\omega}}{2} D_0^s(\omega), \quad (94)$$

$$G_{J_y, J_y}^r(\omega) = \frac{\tilde{G}_{J_y, J_y}^{r,0}(\omega) + V_{\text{ind}}(\omega) \frac{m}{2e^2 \tilde{\omega} N} \left(\tilde{G}_{J_x, J_y}^{r,0}(\omega) \tilde{G}_{J_y, J_x}^{r,0}(\omega) - \tilde{G}_{J_x, J_x}^{r,0}(\omega) \tilde{G}_{J_y, J_y}^{r,0}(\omega) \right)}{1 - V_{\text{ind}}(\omega) \frac{m}{2e^2 \tilde{\omega} N} \tilde{G}_{J_x, J_x}^{r,0}(\omega)}. \quad (95)$$

We will now show that $\tilde{\chi}_{ab,0} = \chi_{ab,0}$ and thus $\tilde{G}_{J_a, J_b}^{r,0} = G_{J_a, J_b}^{r,0}$.

2. Proof that $\tilde{\chi}_{ab,0} = \chi_{ab,0}$

From Eqs. (43) and (75) we see that the mean-field effective Hamiltonian of the electron gas is given by

$$\begin{aligned} H_{\text{eff}}^{\text{MF}} &= \sum_j \frac{(\mathbf{p}_j + m\omega_c y_j \mathbf{e}_x)^2}{2m} + \sum_{i>j} V(\mathbf{r}_i - \mathbf{r}_j) \\ &\quad - 2 \frac{\omega_p^2}{\tilde{\omega}^2} \langle p_x + m\omega_c y \rangle \sum_j \frac{p_{j,x} + m\omega_c y_j}{2m} \\ &\quad + \text{cst.}, \end{aligned} \quad (96)$$

with $\langle p_x + m\omega_c y \rangle = \langle p_{j,x} + m\omega_c y_j \rangle \forall j$. Completing squares yields

$$\begin{aligned} H_{\text{eff}}^{\text{MF}} &= \sum_j \frac{1}{2m} \left(p_{j,x} + m\omega_c y_j - \frac{\omega_p^2}{\tilde{\omega}^2} \langle p_x + m\omega_c y \rangle \right)^2 \\ &\quad + \sum_j \frac{p_{j,y}^2}{2m} + \sum_{i>j} V(\mathbf{r}_i - \mathbf{r}_j) + \text{cst.}. \end{aligned} \quad (97)$$

We can see now that

$$p_{j,x} + m\omega_c y_j - \frac{\omega_p^2}{\tilde{\omega}^2} \langle p_x + m\omega_c y \rangle \propto [x_j, H_{\text{eff}}^{\text{MF}}] \quad (98)$$

and thus

$$\langle p_x + m\omega_c y \rangle \left(1 - \frac{\omega_p^2}{\Omega^2 + \omega_p^2} \right) = 0, \quad (99)$$

which implies that $\langle p_x + m\omega_c y \rangle = 0$ and thus $H_{\text{eff}}^{\text{MF}} = H_m$ and $\tilde{\chi}_{ab,0} = \chi_{ab,0}$. This is a no go theorem, implying that the equilibrium properties of the electron gas are not modified by the cavity. Despite this, the linear response properties, are modified, alternative: as we now discuss.

This implies that $\tilde{G}_{J_a, J_b}^{r,0} = G_{J_a, J_b}^{r,0}$. With this, Equations (93), (94) and (95) provide us with an implicit expression of the current response functions of the electron gas coupled to a cavity in terms of the current response functions of the bare electron gas. This culminates the application of our linear response theory. Obtaining explicit expressions for the current response functions is now just a matter of computing the current response functions of the bare electron gas. We refer to the later as bare current response functions and we compute them in the next section.

D. Computing the bare current response functions

To study the bare 2D electron gas we lean on the reasoning laid out in Ref. [34]. There, they study the same 2D electron gas subject to a perpendicular classical magnetic field and coupled to a cavity (70). They show that the cavity only couples to the center-of-mass coordinates. Furthermore, they show that the center-of-mass and relative coordinate sectors of the Hamiltonian commute. This essentially splits the problem into two, the problem of the relative coordinates unmodified by the cavity, and the problem of the center or mass coupled to the cavity. Note from Eqs. (78) and (79) that the currents also only depend on center-of-mass coordinates. Most importantly, the Coulomb interaction between electrons only depends on the relative coordinates. In summary,

the full problem of a 2D electron gas coupled to a cavity can be broken into the problem of the relative coordinates, subject to Coulomb interactions but decoupled from the cavity, and the problem of an independent center of mass coordinate, which couples to the cavity and is solely responsible for the conduction properties of the electron gas. Consequently, in order to compute bare current response functions, we only need to study the center-of-mass sector of the matter Hamiltonian

$$H_m^{\text{cm}} = \frac{(\mathbf{P} - e\mathbf{A}_{\text{ext}}(\mathbf{R}))^2}{2m}, \quad (100)$$

with $\sqrt{N}\mathbf{R} = \sum_j \mathbf{r}_j$ and $\sqrt{N}\mathbf{P} = \sum_j \mathbf{p}_j$ the center-of-mass position and momentum operators. This is just the Hamiltonian of a single electron under a classical magnetic field, the prototypical example of Landau quantization [39][Chap. 1]. The eigenstates of the system are separable, into plane waves in the X direction and eigenstates of a displaced harmonic oscillator of frequency ω_c along the Y direction

$$\begin{aligned} H_m^{\text{cm}}|K_X, n\rangle &= \omega_c \left(c^\dagger c + \frac{1}{2} \right) |K_X, n\rangle \\ &= \omega_c \left(n + \frac{1}{2} \right) |K_X, n\rangle, \end{aligned} \quad (101)$$

With $P_X|K_X, n\rangle = K_X|K_X, n\rangle$. Here

$$V = \sqrt{\frac{1}{2\omega_c}} (c + c^\dagger), \quad (102)$$

$$P_V = i\sqrt{\frac{\omega_c}{2}} (c^\dagger - c), \quad (103)$$

and $V = \sqrt{m}(Y + K_X l_c^2)$, $P_V = P_Y/\sqrt{m}$, with $l_c = \sqrt{1/(eB)}$.

From the definition in Eq. (77) (ignoring the contribution from the cavity to get the bare current) we can see that the current only depends on center-of-mass coordinates

$$\mathbf{J} = \sqrt{N} \frac{e}{m} (\mathbf{P} - e\mathbf{A}_{\text{ext}}(\mathbf{R})). \quad (104)$$

After some manipulation, we can express

$$J_x = \frac{e\omega_c}{\sqrt{2m}} \left(\frac{1}{\omega_c\sqrt{m}}(P_X - K_X) + \frac{1}{\sqrt{\omega_c}}(c + c^\dagger) \right), \quad (105)$$

$$J_y = i\frac{e\sqrt{\omega_c}}{\sqrt{2m}} (c^\dagger - c), \quad (106)$$

and the matrix elements

$$\begin{aligned} \langle K'_X, n|J_x|K_X, m\rangle &= \delta_{K_X, K'_X} \frac{e\sqrt{\omega_c}}{\sqrt{2m}} (\sqrt{m+1}\delta_{n, m+1} \\ &\quad + \sqrt{m}\delta_{n, m-1}), \end{aligned} \quad (107)$$

$$\begin{aligned} \langle K'_X, n|J_y|K_X, m\rangle &= \delta_{K_X, K'_X} i\frac{e\sqrt{\omega_c}}{\sqrt{2m}} (\sqrt{m+1}\delta_{n, m+1} \\ &\quad - \sqrt{m}\delta_{n, m-1}). \end{aligned} \quad (108)$$

This shows that the current operators are diagonal with respect to the plane waves along the X direction, such that the spectral decomposition of the current response functions can be written simply as a sum over eigenstates of the harmonic oscillator along the Y direction. At zero temperature, this reads

$$G_{J_a, J_b}^{r,0}(\omega) = \sum_n \left(\frac{\langle 0|J_a|n\rangle\langle n|J_b|0\rangle}{\omega_+ + E_0 - E_n} - \frac{\langle n|J_a|0\rangle\langle 0|J_b|n\rangle}{\omega_+ + E_n - E_0} \right). \quad (109)$$

From Eqs. (107), (108) and (109) we obtain the bare current response functions

$$\begin{aligned} G_{J_x, J_x}^{r,0}(\omega) &= G_{J_y, J_y}^{r,0}(\omega) \\ &= -\frac{Ne^2\omega_c}{m} \frac{1}{2} \left(\frac{1}{\omega_+ + \omega_c} - \frac{1}{\omega_+ - \omega_c} \right), \end{aligned} \quad (110)$$

$$G_{J_x, J_y}^{r,0}(\omega) = \frac{Ne^2\omega_c}{m} \frac{i}{2} \left(\frac{1}{\omega_+ + \omega_c} + \frac{1}{\omega_+ - \omega_c} \right), \quad (111)$$

$$G_{J_y, J_x}^{r,0}(\omega) = -\frac{Ne^2\omega_c}{m} \frac{i}{2} \left(\frac{1}{\omega_+ + \omega_c} + \frac{1}{\omega_+ - \omega_c} \right). \quad (112)$$

E. Explicit expressions for the current response functions

Substituting Eqs. (110), (111), (112) and $V_{\text{ind}}(\omega) = \omega_p^2 D_0^s(\omega)$, with $D_0^s(\omega)$ the analytic continuation of $D_0^s(\omega_m)|_{i\omega_m \rightarrow \omega_+}$ (87), into Eqs. (93), (94) and (95) yields, after some manipulation,

$$G_{J_x, J_y}^r(\omega) = i\frac{Ne^2}{m} \frac{\omega_c\omega_+ (\omega_+^2 - \Omega^2)}{(\omega_+^2 - \tilde{\omega}^2) (\omega_+^2 - \omega_c^2) - \omega_p^2\omega_c^2}, \quad (113)$$

$$G_{J_x, J_x}^r(\omega) = \frac{Ne^2}{m} \frac{(\omega_c^2 + \omega_p^2) (\omega_+^2 - \frac{\Omega^2\omega_c^2}{\omega_c^2 + \omega_p^2})}{(\omega_+^2 - \tilde{\omega}^2) (\omega_+^2 - \omega_c^2) - \omega_p^2\omega_c^2}, \quad (114)$$

$$G_{J_y, J_y}^r(\omega) = \frac{Ne^2}{m} \frac{\omega_c^2 (\omega_+^2 - \Omega^2)}{(\omega_+^2 - \tilde{\omega}^2) (\omega_+^2 - \omega_c^2) - \omega_p^2\omega_c^2}. \quad (115)$$

These current response functions have poles at $\omega_+ = \pm\Omega_\pm$, with Ω_\pm the frequencies of the Landau polaritons

$$2\Omega_\pm = \tilde{\omega}^2 + \omega_c^2 \pm \sqrt{(\tilde{\omega}^2 - \omega_c^2)^2 + 4\omega_c^2\omega_p^2}. \quad (116)$$

This is all in agreement with the Landau polaritons and current response functions computed in Ref. [34]. There, they solve the system exactly, computing the energies and wavefunctions and subsequently the current response functions from the spectral decomposition formula. Therefore, the agreement serves as validation that our effective theory correctly predicts the response functions of a material coupled to a cavity. We also recover the dc conductivities in the long-wavelength limit $\Omega \rightarrow 0$, $\delta \rightarrow 0$ of Ref. [33].

For completeness, let us write down the dc ($\omega \rightarrow 0$) conductivities, which are typically of interest when considering the quantum Hall effect,

$$\sigma_{xy} = \frac{e^2\nu}{h} \frac{\omega_c^2(\Omega^2 + \delta^2)}{(\Omega_-^2 + \delta^2)(\Omega_+^2 + \delta^2)}, \quad (117)$$

$$\sigma_{xx} = \sigma_D \left(1 - \frac{(\omega_c^2 + \omega_p^2) \left(\frac{\Omega^2 \omega_c^2}{\omega_c^2 + \omega_p^2} + \delta^2 \right)}{(\Omega_-^2 + \delta^2)(\Omega_+^2 + \delta^2)} \right), \quad (118)$$

$$\sigma_{yy} = \sigma_D \left(1 - \frac{\omega_c^2(\Omega^2 + \delta^2)}{(\Omega_-^2 + \delta^2)(\Omega_+^2 + \delta^2)} \right). \quad (119)$$

Note that $\sigma_D = e^2\rho_{2D}/(m\delta)$ is the Drude dc conductivity and that in σ_{xy} we have introduced the Landau level filling factor $\nu = \rho_{2D}h/(eB)$.

It is also interesting to consider the limit of vanishing classical magnetic field $\omega_c \rightarrow 0$, where the system is just the bare electron gas coupled to a cavity. In this case, we can see from Eqs. (113), (114) and (115) that only G_{J_x, J_x}^r is non-zero. This stems from the fact that all the bare current response functions vanish in this limit, Cf. Eqs (110), (111) and (112). Despite this, G_{J_x, J_x}^r does not vanish because it contains a term that depends solely on the cavity, i.e. the cavity acts as a current channel in the direction of the light-matter coupling independent of whether the material is a conductor or not. This is evidenced by Eq. (91) where the last term solely depends on the free photonic propagator. With this, the optical conductivity reads

$$\sigma_{xx}(\omega) = \sigma_D \frac{i\delta}{\omega_+} \left(1 + \frac{\omega_p^2}{\omega_+^2 - \tilde{\omega}^2} \right). \quad (120)$$

This is in agreement with the optical conductivity of the 2D free electron gas computed in Ref. [15]. Once again, there, they solve the system exactly, computing the energies and wavefunctions and subsequently the current response functions.

V. SPIN MODELS IN A CAVITY

A. Dicke model

We apply now our LRT to the paradigmatic Dicke model [40], for which $H_m = \frac{\omega_z}{2} \sum_j \sigma_j^z$ and $C_x = \sum_j \sigma_j^x$. Here the matter subsystem is just a collection of independent emitters and the only interactions are those mediated by the cavity. Accordingly

$$H_{\text{eff}}^{\text{MF}} = \frac{\omega_z}{2} \sum_j \sigma_j^z + \frac{2\lambda^2(\zeta - 1)}{\Omega} m_x \sum_j \sigma_j^x - \frac{\lambda^2(\zeta - 1)}{\Omega} m_x^2 \quad (121)$$

with $m_x = N^{-1} \langle \sum_j \sigma_j^x \rangle$. Note that for $\zeta = 1$, i.e. in the presence of a P^2 term, the effective term vanishes and $H_{\text{eff}}^{\text{MF}} = H_m$. Otherwise, Hamiltonian (121) can be solved variationally with respect to m_x (See App. B for details) obtaining, at zero temperature,

$$m_x = \begin{cases} 0 & \text{if } \lambda^2(1 - \zeta) \leq \frac{1}{4}\omega_z\Omega, \\ \sqrt{1 - \left(\frac{\Omega\omega_z}{4\lambda^2(1 - \zeta)} \right)^2} & \text{if } \lambda^2(1 - \zeta) > \frac{1}{4}\omega_z\Omega. \end{cases} \quad (122)$$

For $\zeta = 0$ the model exhibits a phase transition between a paramagnetic phase with $m_x = 0$ and a ferromagnetic phase (also termed superradiant when the emphasis is put on the cavity) with $m_x \neq 0$. The response function reads

$$\tilde{\chi}_{xx,0}(\omega) = -\frac{\omega_z^2}{\varepsilon^2} \frac{2\varepsilon}{\omega_+^2 - \varepsilon^2}, \quad (123)$$

with $\varepsilon^2 = \omega_z^2 + \left(\frac{4\lambda^2(1 - \zeta)}{\Omega} m_x \right)^2$. It depends on the value of m_x and thus on the phase.

The photonic propagator, $D(\omega)$, which exhibits poles at the resonant frequencies of the hybrid system [14]. The exact polaritons can be obtained with a two-oscillator solution of the Dicke model in the thermodynamic limit. In the case of $\zeta = 0$, which corresponds to the standard Dicke model, these read [41]

$$2\Omega_{\pm}^2 = \begin{cases} \omega_z^2 + \Omega^2 \pm \sqrt{(\omega_z^2 - \Omega^2)^2 + 16\lambda^2\omega_z\Omega} & \text{if } \lambda^2 \leq \frac{1}{4}\omega_z\Omega, \\ \omega_z^2/\mu^2 + \Omega^2 \pm \sqrt{(\omega_z^2/\mu^2 - \Omega^2)^2 + 4\omega_z^2\Omega^2} & \text{if } \lambda^2 > \frac{1}{4}\omega_z\Omega, \end{cases} \quad (124)$$

with $\mu = \omega_z\Omega/(4\lambda^2)$. In the case of $\zeta = 1$, the same analysis is possible, except in this case there is only a paramagnetic phase due to the presence of the P^2 term. In the two-oscillator solution, the P^2 term affecting the spin becomes an A^2 term of the corresponding oscillator. It can be eliminated with a Bogoliubov transform, yielding a renormalized frequency $\tilde{\omega}_z^2 = \omega_z(\omega_z + 4\lambda^2/\Omega)$ and

coupling $\tilde{\lambda} = \lambda(1 + 4\lambda^2/(\omega_z\Omega))^{-1/4}$. Then, the polaritons are just those of the standard Dicke model in the normal phase (top case of Eq. (124)), with the substitution $\omega_z \rightarrow \tilde{\omega}_z$ and $\lambda \rightarrow \tilde{\lambda}$. For both $\zeta = 0$ and $\zeta = 1$ we find perfect agreement between the exact Dicke polaritons and the poles of the propagator computed with our linear response theory [14].

B. Lipskin-Meshkov-Glick model with longitudinal coupling to the cavity

We consider now the Lipskin-Meshkov-Glick (LMG) model with longitudinal coupling to the cavity as a marginal generalization of the Dicke model. In contrast with the Dicke model, this one incorporates intrinsic all-to-all interactions in the matter subsystem.

The full Hamiltonian reads

$$H = \frac{\omega_z}{2} \sum_j \sigma_j^z - \frac{J}{N} \sum_{ij} \sigma_i^x \sigma_j^x + \Omega a^\dagger a + g(a + a^\dagger) \sum_j \sigma_j^x. \quad (125)$$

Interestingly, the collective nature of the intrinsic interaction allows two alternative treatments within the linear response theory. The first option is to treat it like we would any other intrinsic interaction: bundle it together with the field term to form the matter Hamiltonian, $H_m = \frac{\omega_z}{2} \sum_j \sigma_j^z - \frac{J}{N} \sum_{ij} \sigma_i^x \sigma_j^x$, and then follow the linear response theory as described in Sec. III. The second option exploits the collective nature of the intrinsic interaction and treats this term not within H_m but explicitly within the linear response theory, analogously to the P^2 term, as it is, in fact, just a negative P^2 term [Cf. Eqs. (1) and (125)]. We will follow this second option for its simplicity, since, as we show below, the resulting $H_{\text{eff}}^{\text{MF}}$ corresponds to free spins and is identical in structure to the one from the Dicke model (121). Accordingly, we have

$$V_{\text{ind}}(\omega) = \frac{2\lambda^2}{\Omega} \frac{\Omega^2}{\omega^2 - \Omega^2} - 2J, \quad (126)$$

and

$$H_{\text{eff}}^{\text{MF}} = \frac{\omega_z}{2} \sum_j \sigma_j^z - 2J_{\text{eff}} m_x \sum_j \sigma_j^x + J_{\text{eff}} m_x^2, \quad (127)$$

with $m_x = N^{-1} \langle \sum_j \sigma_j^x \rangle$ and $J_{\text{eff}} = \frac{\lambda^2}{\Omega} + J$. Solving the Hamiltonian variationally with respect to m_x (See App.

B for details) yields, at zero temperature,

$$m_x = \begin{cases} 0 & \text{if } \omega_z \geq 4J_{\text{eff}}, \\ \sqrt{1 - \left(\frac{\omega_z}{4J_{\text{eff}}}\right)^2} & \text{if } \omega_z < 4J_{\text{eff}}. \end{cases} \quad (128)$$

Like the Dicke model (for $\zeta = 0$), the LMG model exhibits a phase transition between a paramagnetic phase with $m_x = 0$ and a ferromagnetic phase with $m_x \neq 0$. The response function reads [26]

$$\tilde{\chi}_{xx,0}(\omega) = -\frac{\omega_z^2}{\varepsilon^2} \frac{2\varepsilon}{\omega_+^2 - \varepsilon^2}, \quad (129)$$

with $\varepsilon^2 = \omega_z^2 + (4J_{\text{eff}} m_x)^2$. It depends on the value of m_x and thus on the phase.

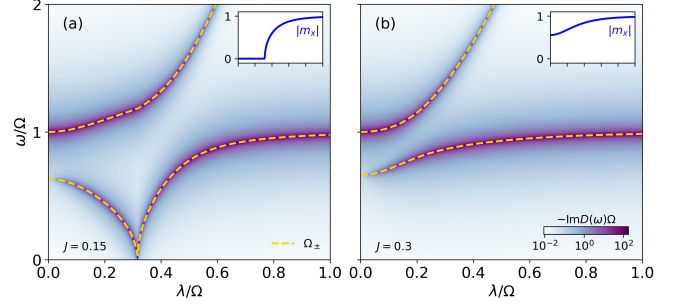


FIG. 1. Cavity response, D , of the LMG model with longitudinal coupling to the cavity as a function of the collective coupling, λ , for different values of the intrinsic interaction, J . The dashed lines correspond to a fit of the polaritons with a two-oscillator model. The top right insets show the magnetization. The transverse field is set to $\omega_z = \Omega$.

In Fig. 1 we show the photonic propagator, $D(\omega)$, which exhibits poles at the resonant frequencies of the hybrid system, as a function of the collective coupling. For $J < \omega_z/4$ the lower mode goes to zero at finite coupling, signaling the phase transition. The critical point is displaced to a lower coupling, λ , with respect to the Dicke model due to the synergy between the intrinsic and effective interactions. For $J > \omega_z/4$ the system is always on the ordered phase independently of the value of λ . In both cases there is a splitting at zero coupling, $\lambda = 0$, due to the intrinsic interactions. In Fig. 1 we also overlay the exact polaritons obtained with a two-oscillator solution of the LMG model in the thermodynamic limit. It is a generalization of the two-oscillator solution of the Dicke model, developed in Ref. [41], to account for the interaction term. The resulting LMG polaritons are

$$2\Omega_{\pm}^2 = \begin{cases} \tilde{\omega}_z^2 + \Omega^2 \pm \sqrt{(\tilde{\omega}_z^2 - \Omega^2)^2 + 16\tilde{\lambda}^2\omega_z\Omega} & \text{if } \omega_z \geq 4J_{\text{eff}}, \\ \omega_z^2/\tilde{\mu}^2 - 4\tilde{\mu}J\omega_z + \Omega^2 \pm \sqrt{(\omega_z^2/\tilde{\mu}^2 - 4\tilde{\mu}J\omega_z + \Omega^2)^2 + 16\lambda^2\tilde{\mu}\omega_z\Omega} & \text{if } \omega_z < 4J_{\text{eff}}, \end{cases} \quad (130)$$

with $\tilde{\omega}_z^2 = \omega_z(\omega_z - 4J)$, $\tilde{\lambda} = \lambda(1 - 4J/\omega_z)^{-1/4}$ and $\tilde{\mu} = \omega_z/(4J_{\text{eff}})$. We find perfect agreement between the exact LMG polaritons and the poles of the propagator computed with our linear response theory.

This model describes recent experiments in rare earth quantum Ising systems, such as LiHoF₄ [21, 22]. These experiments aim to observe how the lowest excitation mode softens as it approaches the ferromagnetic transition. We can understand that Eq. (125) is equivalent to a Dicke model where λ becomes $\sqrt{\lambda^2 + J\Omega}$. Therefore, the softening of the mode can be viewed as the behavior of the lower polariton in the Dicke model.

C. Lipskin-Meshkov-Glick model with transverse coupling to the cavity (Dicke-LMG model)

Thus far we have only considered models where the intrinsic and cavity-mediated interactions are synergistic, here we consider the Dicke-LMG model: an LMG model with transverse coupling to the cavity, named in analogy to the Dicke-Ising model that we will study in the next section. The full Hamiltonian reads

$$H = \frac{\omega_x}{2} \sum_j \sigma_j^x + \frac{\omega_z}{2} \sum_j \sigma_j^z - \frac{J}{N} \sum_{ij} \sigma_i^z \sigma_j^z + \Omega a^\dagger a + g(a + a^\dagger) \sum_j \sigma_j^x. \quad (131)$$

For vanishing longitudinal and transverse fields the Dicke-LMG model has a $\mathbb{Z}_2 \times \mathbb{Z}_2$ symmetry. The first symmetry corresponds to a spin flip, $\sigma_j^z \rightarrow -\sigma_j^z$, and in the bare LMG model it is spontaneously broken in a second order phase transition from a paramagnetic to a ferromagnetic phase. The second symmetry corresponds to a simultaneous cavity-field and spin flip, $a \rightarrow -a$ and $\sigma_j^x \rightarrow -\sigma_j^x$, and in the bare Dicke model

it is spontaneously broken in a second order phase transition from a normal to a superradiant phase. As we show in the following, we find that the combination of the two symmetries gives rise to a first-order phase transition in the Dicke-LMG model between two symmetry-broken phases: a ferromagnetic normal phase for large J and a paramagnetic superradiant phase for large λ^2/Ω , this is akin to what occurs in the Dicke-Ising model (See Sec. VD). Switching on the external field has the effect of explicitly breaking the corresponding symmetry, preventing the spontaneous symmetry breaking that characterizes a phase transition. We find that if only one external field is switched on, the phase transition is demoted from first to second order. If the two external fields are switched on, the phase transition is eliminated completely.

In order to solve the model, we will consider the intrinsic collective interactions explicitly within the linear response theory. However, unlike in the case of the LMG model with longitudinal coupling to the cavity, in this case the cavity-mediated and intrinsic interactions act on different axes, i.e. they couple different collective operators: $C_x = \sum_j \sigma_j^x$ and $C_z = \sum_j \sigma_j^z$ respectively. Accordingly, a slight generalization of the linear response theory presented in Sec. III is required as there are now two induced interaction terms within the effective action

$$V_{\text{ind},x}(\omega) = \frac{2\lambda^2}{\Omega} \frac{\Omega^2}{\omega_+^2 - \Omega^2}, \quad (132)$$

$$V_{\text{ind},z}(\omega) = -2J. \quad (133)$$

Thus, the system can be solved using a multimode generalization of the linear response theory, developed in App. A. The expression for the photonic propagator remains unchanged, see Eq. 30, as it solely determined by the operator that couples to the cavity. In contrast, matter correlators have new contributions afforded by the new interaction channel, $V_{\text{ind},z}$. We find

$$\chi_{xx} = \frac{\tilde{\chi}_{xx,0} + V_{\text{ind},z} \det(\tilde{\chi}_0)}{1 + V_{\text{ind},x} \tilde{\chi}_{xx,0} + V_{\text{ind},z} \tilde{\chi}_{zz,0} + V_{\text{ind},x} V_{\text{ind},z} \det(\tilde{\chi}_0)}, \quad (134)$$

with $(\tilde{\chi}_0)_{ab} = \tilde{\chi}_{ab,0}$. The mean-field effective Hamiltonian reads

$$H_{\text{eff}}^{\text{MF}} = \frac{\tilde{\omega}_x}{2} \sum_j \sigma_j^x + \frac{\tilde{\omega}_z}{2} \sum_j \sigma_j^z + \frac{N\lambda^2}{\Omega} m_x^2 + NJm_z^2, \quad (135)$$

with $\tilde{\omega}_x = \omega_x - 4\frac{\lambda^2}{\Omega} m_x$ and $\tilde{\omega}_z = \omega_z - 4Jm_z$. Solving variationally with respect to m_x and m_z (See App. B for details) allows us to compute the equilibrium values of m_x and m_z numerically and subsequently the response functions $\tilde{\chi}_{xx,0}$, $\tilde{\chi}_{xz,0}$, $\tilde{\chi}_{zx,0}$ and $\tilde{\chi}_{zz,0}$, which depend on the values of m_x and m_z .

In Fig. 2 we show the photonic propagator, $D(\omega)$,

the matter response function, $\chi_{zz}(\omega)$, (left inset) and the magnetizations, m_x and m_z , (right inset) as functions of the collective coupling, λ , in four different scenarios of external fields values. The intrinsic interaction is set so that at zero coupling the cavity and the spins are resonant: $4J = \Omega$. In the case of vanishing ω_x and ω_z , Fig. 2(a), we observe a first order phase transition, evidenced by the discontinuous behaviour in the order parameters of the two ordered phases. The photonic propagator has a pole that goes to zero at the critical point, signaling the gap closing. We include χ_{zz} in the left inset for completeness because the photonic propagator depends on χ_{xx}

[Cf. Eq. (30)] and the system becomes unresponsive to probing along the x direction in the superradiant phase. This is caused by the fact that the intrinsic interaction is the only term in the Hamiltonian containing σ^z operators. Due to its collective nature, its effect is switched off (mean-field behaviour) in the superradiant phase where $m_z = 0$ [Cf. Eq. (135)]. The system is then fully ordered along x and with no off-diagonal terms it becomes unresponsive to probing with σ^x . Accordingly, in the superradiant phase the photonic propagator only shows a pole at the cavity frequency. To witness the other excitation of the system we look at χ_{zz} which shows a pole that emerges from zero at the critical point, signaling the gap reopening. The combination of D and χ_{zz} provides a complete picture of the excitations of the system. In Fig. 2(b) we see that switching on the transverse field, ω_x , eliminates the superradiant symmetry. The phase transition becomes of second order, with m_z the sole order parameter. Like in the previous case, the absence of non mean-field terms containing σ^z in the Hamiltonian makes the system unresponsive to σ_x in the superradiant phase. Thus, we also include χ_{zz} to witness the gap reopening. Alternatively, in Fig. 2(c) we see that switching on the longitudinal field, ω_z , eliminates the ferromagnetic symmetry. The phase transition becomes of second order, with m_x as the sole order parameter. In this case, the presence of the longitudinal field endows the photonic propagator with visibility of all the excitations, showcasing the full gap closing and reopening at the critical point. Finally in Fig. 2(d) we switch on both the longitudinal and transverse fields. All symmetries are now explicitly broken and the phase transition gives way to a smooth crossover of m_z and m_x dominant regimes for small and large λ respectively. The gap remains finite at all times.

D. Ising model with transverse coupling to the cavity (Dicke-Ising model)

Thus far we have only considered models with collective intrinsic interactions, such that despite being intrinsic, these collective interactions were handled on a par with the light-matter interactions using the linear response theory. As a result, the mean-field effective Hamiltonian corresponded to free spins and was trivially solved. Here we consider the Dicke-Ising model: a Ising model with transverse coupling to the cavity [30, 42–44]. The intrinsic interactions are between nearest-neighbours, i.e. not collective, and as such they cannot be handled within the linear response theory like a P^2 term. The full Hamiltonian reads

$$H = \frac{\omega_x}{2} \sum_j \sigma_j^x - J \sum_j \sigma_j^z \sigma_{j+1}^z + \Omega a^\dagger a + g (a + a^\dagger) \sum_j \sigma_j^x. \quad (136)$$

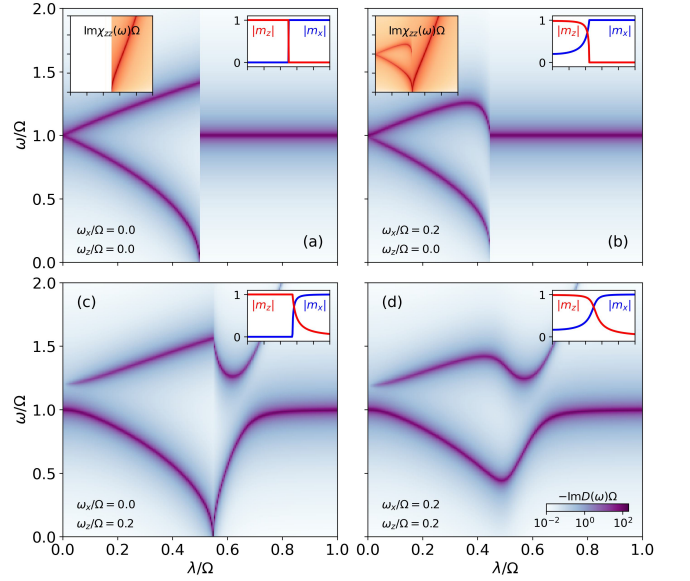


FIG. 2. Cavity response, D , of the Dicke-LMG model (LMG model with transverse coupling to the cavity) as a function of the collective coupling, λ , for different values of the longitudinal and transverse fields, ω_z and ω_x respectively. The top left insets show the matter response χ_{zz} . The top right insets show the magnetizations. The intrinsic interaction is set to $4J = \Omega$.

Like the LMG-Dicke model, and for the same reasons (See Sec. VB), for vanishing transverse field the Dicke-Ising model has a $\mathbb{Z}_2 \times \mathbb{Z}_2$ symmetry that gives rise to a first-order phase transition between two symmetry-broken phases: a ferromagnetic normal phase for large J and a paramagnetic superradiant phase for large λ^2/Ω . However, unlike in the Dicke-LMG model, the phase transition remains of first order after switching on the transverse field. We attribute this robustness to the fact that the intrinsic interactions are not collective in this case. As we will see below, we do not consider a longitudinal field because the resulting mean-field effective Hamiltonian would not be analytically solvable.

The corresponding mean-field effective Hamiltonian is that of a Ising chain in transverse field

$$H_{\text{eff}}^{\text{MF}} = \frac{\tilde{\omega}_x}{2} \sum_j \sigma_j^x - J \sum_j \sigma_j^z \sigma_{j+1}^z + \frac{N\lambda^2}{\Omega} m_x^2, \quad (137)$$

with $\tilde{\omega}_x = \omega_x - 4\lambda^2/\Omega m_x$ and $m_x = N^{-1} \sum_j \langle \sigma_j^x \rangle$. The transverse field is a combination of the external field and the mean-field cavity-induced interaction. It is clear now that adding a longitudinal field would make $H_{\text{eff}}^{\text{MF}}$ analytically intractable. In the thermodynamic limit, $N \rightarrow \infty$, the ground-state energy per spin is given by

$$e_0(m_x) = \frac{\lambda^2}{\Omega} m_x^2 - \frac{1}{2} \int_{-\pi}^{\pi} \frac{dk}{2\pi} \epsilon_k, \quad (138)$$

with

$$\epsilon_k = \sqrt{(2J)^2 + \tilde{\omega}_x^2 - 4J\tilde{\omega}_x \cos k}. \quad (139)$$

Solving variationally allows us to compute the equilibrium value of m_x numerically and subsequently the response function $\tilde{\chi}_{xx,0}$, which depends on the value of m_x . At zero temperature and in the continuum limit, $\tilde{\chi}_{xx,0}$ is given by (See App. C for details)

$$\tilde{\chi}_{xx,0}(\omega) = -32J^2 \int_{-\pi}^{\pi} \frac{dk}{2\pi} \frac{\sin^2 k}{\epsilon_k(\omega^2 - 4\epsilon_k^2)}. \quad (140)$$

Interestingly, we find that $\tilde{\chi}_{xx,0}$ has poles at $2\epsilon_k$. This stems from the fact that

$$C_x = \sum_j \sigma_j^x = N - 2 \sum_k (v_k^2 + (u_k^2 - v_k^2)\gamma_k^\dagger \gamma_k + iu_k v_k (\gamma_k^\dagger \gamma_{-k}^\dagger - \gamma_{-k} \gamma_k)), \quad (141)$$

where γ_k and γ_k^\dagger are the annihilation and creation operators of the Bogoliubov fermions that constitute the elementary excitations of the Ising model after a Jordan-Wigner fermionization, with u_k and v_k the Bogoliubov coefficients [45][Chap. 10]. The physical consequences of this coupling were discussed in Ref. [14]. Here we present a comparison between our LRT and finite-size exact-diagonalization results in Fig. 3. This allows us to discuss how quickly finite-size effects are washed out as we increase the system size and provides another check of our formulas in this non-trivial case.

We compare our LRT in Figs. 3(a), (c) and (e), valid in the thermodynamic limit, with exact-diagonalization results for system sizes up to $N = 14$ in Figs. 3(b), (d) and (f). Let us begin by comparing Figs. 3(a) and (b), which correspond to the case of vanishing classical field. In this case we observe the formation of polaritons in the normal phase and the opening of the two-excitation band and the hardening of the lower polariton in the superradiant phase in Fig. 3(a). The same features are observed in Fig. 3(b), although the two-excitation band is not fully formed and instead we can distinguish a collection of discrete levels. Additionally, there are some finite-size effects. Most prominently, there is a pole corresponding to the single-excitation band in the normal phase, at $\omega = 2J = \Omega/2$ for $\lambda \rightarrow 0$. This is explained by noting that the coupling operator C_x can create domain walls at the edges of the chain, something which is impossible in the thermodynamic limit, an effect that becomes negligible as $N \rightarrow \infty$. This interpretation is confirmed by the bottom right inset in Fig. 3(b), which shows that the intensity of this pole decreases with size, unlike the poles corresponding to the polaritons. Figures 3(c), (d), (e) and (f) feature a finite classical field ω_x and thus a finite bandwidth in the normal phase. In Fig. 3(c) the narrow bandwidth allows the formation of bound polariton states (BPS) with well defined energies below and above the band [14]. This is validated in Fig. 3(d). Again, we observe additional features that we attribute to finite size-effects. In particular the single-excitation band, at $\omega = 2J = \Omega/2$ for $\lambda \rightarrow 0$. Its visibility is shown to decrease with size in the bottom right inset of Fig. 3(d). In

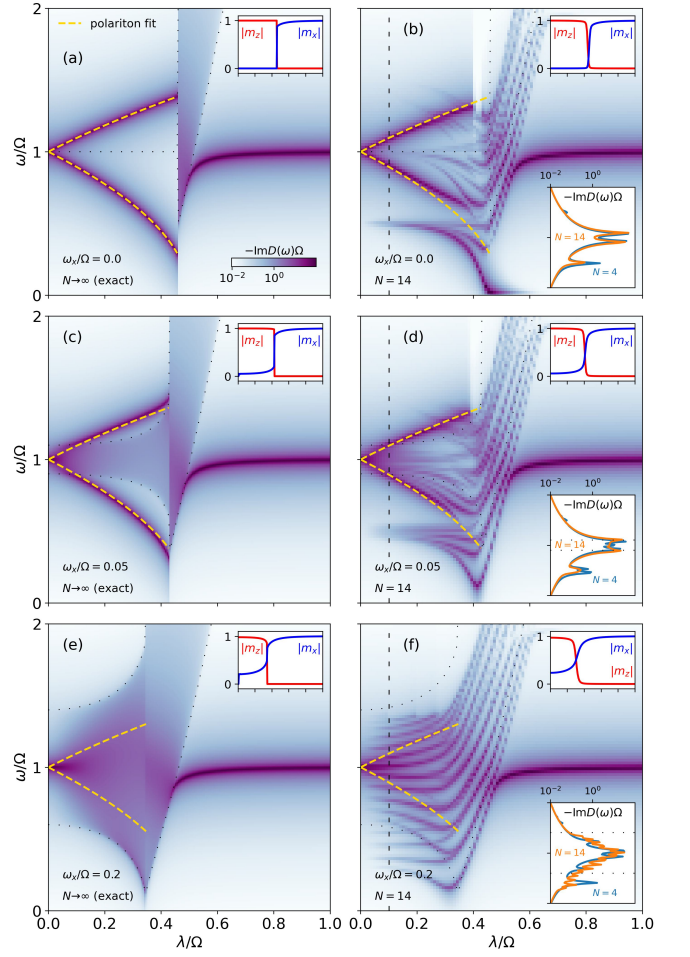


FIG. 3. Cavity response, D , of the Dicke-Ising model as a function of the collective coupling, λ , computed analytically in the thermodynamic limit, $N \rightarrow \infty$, (left) and with exact diagonalization, $N = 14$, (right) for different values of the classical field, ω_x . The yellow dashed lines correspond to a fit of the polaritons with a two-oscillator model. The top right insets show the magnetizations. The bottom right inset in the right plots shows a vertical cut at the black dashed line for two finite sizes, $N = 4$ and $N = 14$. The dotted lines mark the edges of the band of the mean-field effective Hamiltonian (137). The parameters are $\omega_x = 0$ and $4J = \Omega$. In the exact-diagonalization results, the Fock basis for the photonic Hilbert space is truncated at 40 photons.

Fig. 3(e) the large bandwidth prevents the formation for BPS. This is confirmed in Fig. 3(f) where we observe a collection of closely packed levels of equal visibility that are expected to form the band in the thermodynamic limit. There are not any two levels that stand out as polaritons, in agreement with our LRT. The levels that fall outside the would-be band are shown to be finite-size artifacts in the bottom right inset of Fig. 3(f).

E. Heisenberg ferromagnet coupled to a cavity

We finish the section by commenting on the paradigmatic Heisenberg model. In particular we consider a ferromagnetic Heisenberg model on a 3D lattice, such that the model is ordered below a critical temperature,

$$H_m = -J \sum_{\langle ij \rangle} \boldsymbol{\sigma}_i \boldsymbol{\sigma}_j + \frac{\omega_z}{2} \sum_j \sigma_j^z. \quad (142)$$

The ground state of the model corresponds to a symmetry broken ferromagnetic state. For vanishing field, $\omega_z = 0$, the spins will be magnetized in a random direction of space, spontaneously breaking the $SO(3)$ symmetry of the model. The addition of a field demotes the symmetry to $SO(2)$ in the plane perpendicular to the field, setting the magnetization direction along the field. It also opens a gap between the spin-wave band and the ground state, such that the zero momentum spin-wave has an energy gap with respect to the ground state of ω_z . The coupling to a cavity in a direction perpendicular to the classical field will demote the remaining $SO(2)$ symmetry to \mathbb{Z}_2 in the cavity field direction. The cavity coupling, $C_x = \sum_j \sigma_j^x$, will compete with the classical field in setting the magnetization direction. The corresponding effective Hamiltonian reads

$$H_{\text{eff}}^{\text{MF}} = \frac{\omega_z}{2} \sum_j \sigma_j^z - J \sum_{\langle ij \rangle} \boldsymbol{\sigma}_i \boldsymbol{\sigma}_j - \frac{2\lambda^2}{\Omega} m_x \sum_j \sigma_j^x + \frac{\lambda^2}{\Omega} m_x^2 \quad (143)$$

If we assume that the model is ordered, the interaction term contributes an energy $-Jz$ with z the coordination number, independently of the value of m_x . Thus, the variational Hamiltonian is equivalent to that of a Dicke model [Cf. Sec. V A.]. The behaviour of the magnetization, m_x , is also inherited from the Dicke model. For a subcritical coupling, $\lambda < \sqrt{\omega_z \Omega}/2$, the model is ordered along z . When the coupling reaches the critical point, the magnetization starts to turn towards the x axis in a second order phase transition.

The response function $\tilde{\chi}_{xx,0}$ corresponds to the excitation of the zero-momentum magnon, with a pole at $\omega^2 = \omega_z^2 + (4\lambda^2 m_x / \Omega)^2$. Therefore, our LRT predicts the formation of polaritons of this zero-momentum magnon with frequencies given by Eq. 124, following the physics of the Dicke model.

VI. CONCLUSIONS

In this paper, we have presented a linear response theory for materials collectively coupled to a cavity. We have employed two different approaches. The first relies on a path integral formulation of the partition function and a saddle point expansion of the partition function that is

truncated exactly in the thermodynamic limit. The second is more direct and relies on formulating the equations of motion for the response functions. These are truncated to second order in light-matter fluctuations and solved, yielding equivalent expressions for the response functions to the first approach. This provides a posteriori validation for the truncation of the equations of motion, which confirms the validity of a mean-field decoupling of the light-matter interaction in cavity QED materials. We obtain exact expressions for the response functions of the hybrid system in terms of the bare response functions of the cavity and the material.

The theory has been demonstrated in several systems, showcasing its applicability. In the Quantum Hall effect we have recovered the optical response and Landau polaritons computed previously in Refs. [33, 34]. In magnetic systems, we have started from the non-interacting Dicke model and progressively complicated the model by adding collective intrinsic interactions to yield the LMG model with longitudinal coupling to the cavity, then changing the cavity coupling direction to induce a competition between intrinsic and light-matter interactions in the Dicke-LMG model and finally making the intrinsic interactions non-collective in the Dicke-Ising model. Finally, we have explored the effect of the cavity in an ordered Heisenberg ferromagnet. Our predictions have been validated against analytical and exact-diagonalization results.

Even if the focus of the paper has been the linear response theory, the study of the different spin models has provided some interesting independent physical insights. In particular that first order phase transitions arise in hybrid systems with competing orders, such as the Dicke-LMG and Dicke-Ising models, when the competing constituents feature second-order phase transitions by themselves. In this sense, our results also point to the fact that the robustness of this first order phase transition depends on the nature of the intrinsic material interactions. A transverse field demotes the phase transition to second order for the Dicke-LMG model (collective interactions) but not for the Dicke-Ising model (nearest-neighbor interactions). We underline that this has been witnessed through the lens of the photonic response, which is relevant for its experimental implications. Cavity transmission is a common probing mechanism for magnetic materials inductively coupled to a cavity [46–50]. Finally, the finite-size exact-diagonalization results allow us to gauge what the commonly-used “thermodynamic limit” means in terms of actual system sizes. As shown in Sec. V D, all the features (bar the blending of discrete levels to form the band) expected in the thermodynamic limit are already present for $N = 14$.

Although not explored here, the computation of finite-size corrections is possible. In the path-integral approach this would be achieved by considering higher order terms in the saddle-point expansion. Alternatively, one could truncate the equations of motion at higher order, to include three- or higher-order correlators [51–53]. This

would be relevant in the study of topological systems, where boundary effects are crucial [54–56]. Also, real time dynamics could be easily studied with the framework of the equations of motion [57]. In conclusion, our work lays the foundations of a linear response theory for cavity QED materials.

Appendix A: Linear response theory for a multimode cavity

Consider the Hamiltonian for a material coupled collectively to a multimode cavity

$$H = H_m + \sum_k \Omega_k a_k^\dagger a_k + \sum_k g_k (a_k + a_k^\dagger) C_k + \zeta \sum_k \frac{g_k^2}{\Omega_k} C_k^2. \quad (\text{A1})$$

The corresponding action reads

$$S = S_m + \sum_k \int_\tau \bar{a}_k(\tau) (\partial_\tau - \Omega_k) a_k(\tau) + \sum_k g_k \int_\tau (a_k(\tau) + \bar{a}_k(\tau)) C_k(\tau) + \zeta \sum_k \frac{g_k^2}{\Omega_k} \int_\tau C_k^2(\tau). \quad (\text{A2})$$

After partial integration over the cavity field, the induced action reads

$$S_{\text{ind}} = \frac{1}{2} \sum_{k, \tau, \tau'} C_k(\tau) \frac{1}{N} V_{\text{ind},k}(\tau - \tau') C_k(\tau'), \quad (\text{A3})$$

with

$$V_{\text{ind},k}(\omega_m) = 2\lambda_k^2 \frac{\Omega_k^2(\zeta - 1) + \zeta\omega_m^2}{\Omega_k(\omega_m^2 + \Omega_k^2)}. \quad (\text{A4})$$

Here $D_{k,0}$ is the free photon propagator of the k -th mode

$$D_{k,0}(\omega_m) = \frac{1}{i\omega_m - \Omega_k}. \quad (\text{A5})$$

The induced interaction can be decoupled with a Hubbard-Stratonovich transformation that introduces an auxiliary scalar field for each mode, φ_k :

ACKNOWLEDGEMENTS

We acknowledge discussions with Katharina Lenk, Martin Eckstein, Andreas Wipf, Yuto Ashida, Luis Martín-Moreno, Fernando Falceto and José G. Esteve. Despite the enormous impediments in spending the budget, the authors must acknowledge funding from the grant TED2021-131447B-C21 funded by MCIN/AEI/10.13039/501100011033 and the EU ‘NextGenerationEU’/PRTR. We also acknowledge the Gobierno de Aragón (Grant E09-17R Q-MAD), Quantum Spain and the CSIC Quantum Technologies Platform PTI-001. J. R-R acknowledges support from the Ministry of Universities of the Spanish Government through the grant FPU2020-07231.

$$e^{-S_{\text{ind}}} = \frac{1}{Z_\varphi} \int_\varphi e^{-\frac{1}{2}N \sum_k \int_{\tau, \tau'} \varphi_k(\tau) V_{\text{ind},k}^{-1}(\tau - \tau') \varphi_k(\tau') - i \sum_k \int_\tau \varphi_k(\tau) C_k(\tau)}. \quad (\text{A6})$$

We define the propagator of the auxiliary fields as

$$W_{kp}(\tau) = \langle \varphi_k(\tau) \varphi_p(0) \rangle^c. \quad (\text{A7})$$

The generating functional for bare connected correlation functions of the matter coupling operators, C_k , is $\mathcal{G}_m^0[\xi_k] = -N^{-1} \log Z_m[\xi_k]$ with

$$Z_m[\xi_k] = \int_c e^{-(S_m + i \sum_k \int_\tau \xi_k(\tau) C_k(\tau))}, \quad (\text{A8})$$

such that

$$\begin{aligned} \frac{\delta}{\delta \xi_{k_1}(\tau_1)} \cdots \frac{\delta}{\delta \xi_{k_n}(\tau_n)} \mathcal{G}_m^0[\xi_k] \Big|_{\xi_k=0} &= \\ &= -\frac{(-i)^n}{N} \langle C_{k_1}(\tau_1) \cdots C_{k_n}(\tau_n) \rangle_m^c \\ &\equiv \chi_{k_1 \dots k_n, 0}^{(n)}(\tau_1, \dots, \tau_n). \end{aligned} \quad (\text{A9})$$

In the following we will denote $\chi_{kp,0}^{(2)} \equiv \chi_{kp,0}$. With this, after partial integration over the matter degrees of free-

dom, we can write

$$Z = \oint_{\varphi_k} e^{-Nf[\varphi_k]}, \quad (\text{A10})$$

with

$$f[\varphi_k] = \frac{1}{2} \sum_k \int_{\tau, \tau'} \varphi_k(\tau) V_{\text{ind},k}^{-1}(\tau - \tau') \varphi_k(\tau') + \mathcal{G}_m^0[\varphi_k]. \quad (\text{A11})$$

Like in the single-mode case, we apply a saddle-point approximation for large N . This requires that the number of modes, M , be finite, i.e. that $\lim_{N \rightarrow \infty} M/N \rightarrow 0$. Otherwise higher order terms in the saddle-point expansion might not actually be negligible. The condition that the functional derivatives of f with respect to φ_k vanish

$$\varphi_{k,\text{sp}}(\omega_m) = -\frac{i}{N} V_{\text{ind},k}(\omega_m) \langle C_k(\omega_m) \rangle_{\varphi_{k,\text{sp}}} \quad (\text{A12})$$

formally defines $\varphi_{k,\text{sp}}$. Making the simplifying assumption that $\varphi_{k,\text{sp}}$ be constant we find

$$\varphi_{k,\text{sp}} = -\frac{i}{N} V_{\text{ind},k}(\omega_m = 0) \langle C_k \rangle_{\varphi_{k,\text{sp}}}. \quad (\text{A13})$$

This tells us that $\varphi_{k,\text{sp}}$ is self-consistently proportional to $\langle C_x \rangle_{\varphi_{k,\text{sp}}}$, i.e. to the expectation value of C_k for the bare matter subject to fields $i\varphi_{k,\text{sp}} = \frac{1}{N} V_{\text{ind},k}(\omega_m = 0) \langle C_k \rangle$. This is precisely the self-consistent condition that arises from computing $\langle C_k \rangle$ from the mean-field Hamiltonian

$$H_{\text{eff}}^{\text{MF}} = H_m + \sum_k \frac{2\lambda_k^2(\zeta - 1)}{N\Omega_k} \langle C_k \rangle C_k - \sum_k \frac{\lambda_k^2(\zeta - 1)}{N\Omega_k} \langle C_k \rangle^2. \quad (\text{A14})$$

This is the mean-field theory of the effective Hamiltonian that arises from taking the static limit in $V_{\text{ind},k}$ in the effective action [8].

Expanding f around the saddle-point yields

$$(NW_0)_{kp}^{-1} = \delta_{kp} V_{\text{ind},k}^{-1} + \tilde{\chi}_{kp,0}, \quad (\text{A15})$$

with

$$\begin{aligned} \tilde{\chi}_{kp,0}(\tau_1, \tau_2) &= \frac{\delta}{\delta\varphi_{k,\text{sp}}(\tau_1)} \frac{\delta}{\delta\varphi_{p,\text{sp}}(\tau_2)} \mathcal{G}_m^0 \\ &= \frac{1}{N} \langle C_k(\tau) C_p(\tau') \rangle_{\varphi_{k,\text{sp}}}^c. \end{aligned} \quad (\text{A16})$$

For $N \rightarrow \infty$ one can safely truncate the saddle-point expansion to second order, which implies that $W = W_0$.

We can now obtain relations between the auxiliary field propagator, W_{kp} , the photonic propagator, D_k , and matter response functions. Let us define the generating functional for photonic connected correlators by introducing a complex fields in Eq. (A2): $\mathcal{G}_{\text{ph}}[\eta_k, \bar{\eta}_k] = -\log Z[\eta_k, \bar{\eta}_k]$, with

$$Z[\eta_k, \bar{\eta}_k] = \oint_{a_k, \bar{a}_k, c} e^{-(S + \sum_k \int_{\tau} (a_k(\tau) \bar{\eta}_k(\tau) + \bar{a}_k(\tau) \eta_k(\tau))}. \quad (\text{A17})$$

After partial integration of the cavity fields, this yields

$$\begin{aligned} Z[\eta_k, \bar{\eta}_k] &= \oint_c \exp - \left(S_m + \zeta \sum_k \frac{g_k^2}{\Omega_k} \int_{\tau} C_k^2(\tau) \right. \\ &\quad \left. + \sum_k \int_{\tau, \tau'} \bar{m}_k(\tau) D_k(\tau - \tau') m_k(\tau) \right), \end{aligned} \quad (\text{A18})$$

with $m_k(\tau) = \eta_k(\tau) + g_k C_k(\tau)$. With this

$$D_k(\omega_m) = D_{k,0}(\omega_m) - \lambda_k^2 D_{k,0}(\omega_m) \chi_{kk}(\omega_m) D_{k,0}(\omega_m). \quad (\text{A19})$$

Likewise, we can define the generating functional for matter connected correlators: $\mathcal{G}_m[\xi_k] = -N^{-1} \log Z[\xi_k]$ with

$$Z[\xi_k] = \oint_{c, \varphi_k} e^{-(S_{\text{eff}} + i \sum_k \int_{\tau} \xi_k(\tau) C_k(\tau))}. \quad (\text{A20})$$

After partial integration over the cavity fields, this yields

$$Z[\xi_k] = \oint_{\varphi_k} e^{-Nf[\xi_k + \varphi_k]} \quad (\text{A21})$$

Then, a second order expansion of $f[\xi_k + \varphi_k]$ around the saddle point yields

$$\begin{aligned} f[\xi_k + \varphi_k] - f[\varphi_{k,\text{sp}}] &= \frac{1}{2} \sum_{k,p} \int_{\tau, \tau'} \left(\delta\varphi_k(\tau) (NW)_{kp}^{-1}(\tau - \tau') \delta\varphi_p(\tau') + \xi_k(\tau) \tilde{\chi}_{kp,0}(\tau - \tau') \xi_p(\tau') \right. \\ &\quad \left. + \delta\varphi_k(\tau) \tilde{\chi}_{kp,0}(\tau - \tau') \xi_p(\tau') + \xi_k(\tau) \tilde{\chi}_{kp,0}(\tau - \tau') \delta\varphi_p(\tau) \right). \end{aligned} \quad (\text{A22})$$

The functional integral over the auxiliary-field displacements $\delta\varphi_k$ is just an M -dimensional Gaussian integral that we can perform, yielding

$$G_m[\xi_k] = \text{cst.} + \frac{1}{2} \sum_{k,p} \int_{\tau, \tau'} \xi_k(\tau) \left(\tilde{\chi}_{kp,0}(\tau - \tau') - \sum_{k',p'} \int_{u,v} \tilde{\chi}_{kk',0}(\tau - u) NW_{k'p'}(u - v) \tilde{\chi}_{p'p,0}(v - \tau') \right) \xi_p(\tau'). \quad (\text{A23})$$

With this

$$\chi_{kp}(\omega_m) = \tilde{\chi}_{kp,0}(\omega_m) - \sum_{k',p'} \tilde{\chi}_{kk',0}(\omega_m) NW_{k'p'}(\omega_m) \tilde{\chi}_{p'p,0}(\omega_m). \quad (\text{A24})$$

Note that obtaining final expressions for $\chi_{kp}(\omega_m)$ requires inverting the matrix $(NW)^{-1}$ that is defined in Eq. (A15).

Appendix B: A spin subject to variational fields

1. Spectrum and response functions of a free spin

Let us consider the following free spin model

$$H = \frac{\omega_x}{2} \sigma_x + \frac{\omega_z}{2} \sigma_z. \quad (\text{B1})$$

It is diagonalized by a rotation that defines spin operators along new directions

$$\sigma'_z = \frac{\omega_z}{\epsilon} \sigma_z - \frac{\omega_x}{\epsilon} \sigma_x, \quad (\text{B2})$$

$$\sigma'_x = \frac{\omega_x}{\epsilon} \sigma_z + \frac{\omega_z}{\epsilon} \sigma_x, \quad (\text{B3})$$

$$(\text{B4})$$

where $\epsilon^2 = \omega_x^2 + \omega_z^2$. With these, the Hamiltonian reads

$$H = \frac{\epsilon}{2} \sigma'_z, \quad (\text{B5})$$

with ground-state energy $E_0 = -\epsilon/2$.

We compute the response functions from their spectral decomposition, which, at zero temperature, reads

$$\chi_{ab}(\omega) = - \sum_n \left(\frac{\langle 0 | \sigma_a | n \rangle \langle n | \sigma_b | 0 \rangle}{\omega^+ + E_0 - E_n} - \frac{\langle n | \sigma_a | 0 \rangle \langle 0 | \sigma_b | n \rangle}{\omega^+ + E_n - E_0} \right), \quad (\text{B6})$$

where the sum is over the eigenstates of the system. With the matrix elements

$$\langle n | \sigma_x | 0 \rangle = -\frac{\omega_x}{\epsilon}, \quad (\text{B7})$$

$$\langle n | \sigma_z | 0 \rangle = \frac{\omega_z}{\epsilon}, \quad (\text{B8})$$

we obtain

$$\chi_{xx}(\omega) = -\frac{\omega_z^2}{\epsilon^2} \frac{2\epsilon}{\omega_+^2 - \epsilon^2}, \quad (\text{B9})$$

$$\chi_{xz}(\omega) = \chi_{zx}(\omega) = -\frac{\omega_x \omega_z}{\epsilon^2} \frac{2\epsilon}{\omega_+^2 - \epsilon^2}, \quad (\text{B10})$$

$$\chi_{zz}(\omega) = -\frac{\omega_x^2}{\epsilon^2} \frac{2\epsilon}{\omega_+^2 - \epsilon^2}. \quad (\text{B11})$$

2. Considering variational fields

There will be situations in which we arrive to a free spin model like the one defined in Eq. (B1) from a mean field

approximation. As a result we will have a Hamiltonian of the form

$$H(m_x, m_z) = \frac{\tilde{\omega}_x}{2} \sigma_x + \frac{\tilde{\omega}_z}{2} \sigma_z + E(m_x, m_z), \quad (\text{B12})$$

where now the fields, $\tilde{\omega}_x$ and $\tilde{\omega}_z$ depend on mean-field parameters $m_{a \in \{x,z\}} = \langle \sigma_a \rangle$ and there is a constant energy term that also depends on the variational parameters. The Hamiltonian can be diagonalized as explained in the previous section, and the ground state energy and response functions are now functions of m_x and m_z . In particular, $E_0(m_x, m_z) = -\epsilon(m_x, m_z)/2 + E_0(m_x, m_z)$, with $\epsilon^2 = \tilde{\omega}_x^2 + \tilde{\omega}_z^2$. The values of m_x and m_z are determined variationally from a minimization of $E_0(m_x, m_z)$. Depending on the particular problem, this can be done analytically or numerically.

Appendix C: Computing $\tilde{\chi}_{xx,0}$ for the Ising model

The spectral decomposition of $\tilde{\chi}_{xx,0}$ reads

$$\tilde{\chi}_{xx,0} = -\frac{1}{N} \sum_n |\langle n | C_x | 0 \rangle|^2 \frac{2(E_n - E_0)}{\omega_+^2 - (E_n - E_0)^2}, \quad (\text{C1})$$

where $|n\rangle$ is the eigenstate of $H_{\text{eff}}^{\text{MF}}$ (137) with eigenvalue E_n . From Eq. (141) we see that

$$\langle n | C_x | 0 \rangle = \delta_{n0} \left(N + \sum_k v_k^2 \right) - 2i \sum_k u_k v_k \langle n | \gamma_k^\dagger \gamma_{-k}^\dagger | 0 \rangle, \quad (\text{C2})$$

with [45][Chap. 10]

$$u_k = \sin(\theta_k/2), \quad (\text{C3})$$

$$v_k = \cos(\theta_k/2), \quad (\text{C4})$$

$$\tan \theta_k = \frac{\sin k}{\frac{\tilde{\omega}_x}{2J} - \cos k}. \quad (\text{C5})$$

With this, we find

$$\tilde{\chi}_{xx,0} = -\frac{16J^2}{N} \sum_k \frac{\sin^2 k}{\epsilon_k (\omega_+^2 - 4\epsilon_k^2)} \quad (\text{C6})$$

and in the thermodynamic limit, $\lim_{N \rightarrow \infty} N^{-1} \sum_k f_k = \int_{-\pi}^{\pi} dk / (2\pi) f_k$, we obtain Eq. (140).

-
- [1] A. Altland and B. D. Simons, *Condensed Matter Field Theory* (Cambridge University Press, 2010).
- [2] F. Schlawin, D. M. Kennes, and M. A. Sentef, Cavity quantum materials, *Appl. Phys. Rev.* **9**, 011312 (2022).
- [3] F. J. Garcia-Vidal, C. Ciuti, and T. W. Ebbesen, Manipulating matter by strong coupling to vacuum fields, *Science* **373**, eabd0336 (2021).
- [4] J. Bloch, A. Cavalleri, V. Galitski, M. Hafezi, and A. Rubio, Strongly correlated electron–photon systems, *Nature* **606**, 41–48 (2022).
- [5] K. Hepp and E. H. Lieb, On the superradiant phase transition for molecules in a quantized radiation field: the dicke maser model, *Ann. Phys.* **76**, 360 (1973).
- [6] Y. K. Wang and F. T. Hioe, Phase transition in the dicke model of superradiance, *Phys. Rev. A* **7**, 831 (1973).
- [7] G. M. Andolina, F. M. D. Pellegrino, V. Giovannetti, A. H. MacDonald, and M. Polini, Cavity quantum electrodynamics of strongly correlated electron systems: A no-go theorem for photon condensation, *Phys. Rev. B* **100**, 121109 (2019).
- [8] J. Román-Roche and D. Zueco, Effective theory for matter in non-perturbative cavity QED, *SciPost Phys. Lect. Notes* , 50 (2022).
- [9] M. Moshe and J. Zinn-Justin, Quantum field theory in the large n limit: a review, *Phys. Rep.* **385**, 69–228 (2003).
- [10] G. L. Paravicini-Bagliani, F. Appugliese, E. Richter, F. Valmorra, J. Keller, M. Beck, N. Bartolo, C. Rössler, T. Ihn, K. Ensslin, C. Ciuti, G. Scalari, and J. Faist, Magneto-transport controlled by landau polariton states, *Nat. Phys.* **15**, 186–190 (2018).
- [11] F. Appugliese, J. Enkner, G. L. Paravicini-Bagliani, M. Beck, C. Reichl, W. Wegscheider, G. Scalari, C. Ciuti, and J. Faist, Breakdown of topological protection by cavity vacuum fields in the integer quantum hall effect, *Science* **375**, 1030–1034 (2022).
- [12] A. Thomas, E. Devaux, K. Nagarajan, G. Rogez, M. Seidel, F. Richard, C. Genet, M. Drillon, and T. W. Ebbesen, Large enhancement of ferromagnetism under a collective strong coupling of ybco nanoparticles, *Nano Lett.* **21**, 4365–4370 (2021).
- [13] G. Jarc, S. Y. Mathengattil, A. Montanaro, F. Giusti, E. M. Rigoni, R. Sergo, F. Fassoli, S. Winnerl, S. Dal Zilio, D. Mihailovic, P. Prelovšek, M. Eckstein, and D. Fausti, Cavity-mediated thermal control of metal-to-insulator transition in 1t-tas₂, *Nature* **622**, 487–492 (2023).
- [14] In preparation.
- [15] V. Rokaj, M. Ruggenthaler, F. G. Eich, and A. Rubio, Free electron gas in cavity quantum electrodynamics, *Phys. Rev. Res.* **4**, 013012 (2022).
- [16] J. Li, D. Golez, G. Mazza, A. J. Millis, A. Georges, and M. Eckstein, Electromagnetic coupling in tight-binding models for strongly correlated light and matter, *Phys. Rev. B* **101**, 205140 (2020).
- [17] G. Arwas and C. Ciuti, Quantum electron transport controlled by cavity vacuum fields, *Phys. Rev. B* **107**, 045425 (2023).
- [18] O. Dmytruk and M. Schiró, Gauge fixing for strongly correlated electrons coupled to quantum light, *Phys. Rev. B* **103**, 075131 (2021).
- [19] M. Schuler, D. D. Bernardis, A. M. Läuchli, and P. Rabl, The vacua of dipolar cavity quantum electrodynamics, *SciPost Phys.* **9**, 066 (2020).
- [20] V. Rokaj, D. M. Welakuh, M. Ruggenthaler, and A. Rubio, Light–matter interaction in the long-wavelength limit: no ground-state without dipole self-energy, *J. Phys. B: At. Mol. Opt. Phys.* **51**, 034005 (2018).
- [21] M. Libersky, R. D. McKenzie, D. M. Silevitch, P. C. E. Stamp, and T. F. Rosenbaum, Direct observation of collective electronuclear modes about a quantum critical point, *Phys. Rev. Lett.* **127**, 207202 (2021).
- [22] R. D. McKenzie, M. Libersky, D. M. Silevitch, and T. F. Rosenbaum, Theory of magnon polaritons in quantum ising materials, *Phys. Rev. A* **106**, 043716 (2022).
- [23] J. Román-Roche, F. Luis, and D. Zueco, Photon condensation and enhanced magnetism in cavity qed, *Phys. Rev. Lett.* **127**, 167201 (2021).
- [24] R. Feynman and F. Vernon, The theory of a general quantum system interacting with a linear dissipative system, *Ann. Phys. (N. Y.)* **24**, 118–173 (1963).
- [25] H. Grabert, P. Schramm, and G.-L. Ingold, Quantum brownian motion: The functional integral approach, *Phys. Rep.* **168**, 115 (1988).
- [26] K. Lenk, J. Li, P. Werner, and M. Eckstein, Collective theory for an interacting solid in a single-mode cavity (2022), arXiv:2205.05559.
- [27] C. Gardiner and P. Zoller, *Quantum Noise: A Handbook of Markovian and Non-Markovian Quantum Stochastic Methods with Applications to Quantum Optics*, Springer Series in Synergetics (Springer, 2004).
- [28] E. del Valle, F. P. Laussy, and C. Tejedor, Luminescence spectra of quantum dots in microcavities. ii. fermions, *Phys. Rev. B* **79**, 235326 (2009).
- [29] F. Carollo and I. Lesanovsky, Exactness of mean-field equations for open dicke models with an application to pattern retrieval dynamics, *Phys. Rev. Lett.* **126**, 230601 (2021).
- [30] C. F. Lee and N. F. Johnson, First-order superradiant phase transitions in a multiqubit cavity system, *Phys. Rev. Lett.* **93**, 083001 (2004).
- [31] K. Lenk, J. Li, P. Werner, and M. Eckstein, Dynamical mean-field study of a photon-mediated ferroelectric phase transition, *Phys. Rev. B* **106**, 245124 (2022).
- [32] C. Ciuti, Cavity-mediated electron hopping in disordered quantum hall systems, *Phys. Rev. B* **104**, 155307 (2021).
- [33] V. Rokaj, M. Penz, M. A. Sentef, M. Ruggenthaler, and A. Rubio, Polaritonic hofstadter butterfly and cavity control of the quantized hall conductance, *Phys. Rev. B* **105**, 205424 (2022).
- [34] V. Rokaj, J. Wang, J. Sous, M. Penz, M. Ruggenthaler, and A. Rubio, Weakened topological protection of the quantum hall effect in a cavity, *Phys. Rev. Lett.* **131**, 196602 (2023).
- [35] K. von Klitzing, The quantized hall effect, *Rev. Mod. Phys.* **58**, 519 (1986).
- [36] K. von Klitzing, T. Chakraborty, P. Kim, V. Madhavan, X. Dai, J. McIver, Y. Tokura, L. Savary, D. Smirnova, A. M. Rey, C. Felser, J. Gooth, and X. Qi, 40 years of the quantum hall effect, *Nat. Rev. Phys.* **2**, 397–401 (2020).
- [37] R. Kubo, Statistical-mechanical theory of irreversible processes. i. general theory and simple applications to

- magnetic and conduction problems, *J. Phys. Soc. Jpn.* **12**, 570–586 (1957).
- [38] G. Giuliani and G. Vignale, *Quantum Theory of the Electron Liquid* (Cambridge University Press, 2005).
- [39] D. Tong, Lectures on the quantum hall effect (2016), [arXiv:1606.06687](https://arxiv.org/abs/1606.06687) [hep-th].
- [40] R. H. Dicke, Coherence in spontaneous radiation processes, *Phys. Rev.* **93**, 99 (1954).
- [41] C. Emary and T. Brandes, Chaos and the quantum phase transition in the dicke model, *Phys. Rev. E* **67**, 066203 (2003).
- [42] S. Gammelmark and K. Mølmer, Phase transitions and heisenberg limited metrology in an ising chain interacting with a single-mode cavity field, *New J. Phys.* **13**, 053035 (2011).
- [43] E. Cortese, L. Garziano, and S. De Liberato, Polaron spectrum of the dicke-ising model, *Phys. Rev. A* **96**, 053861 (2017).
- [44] J. Rohn, M. Hörmann, C. Genes, and K. P. Schmidt, Ising model in a light-induced quantized transverse field, *Phys. Rev. Res.* **2**, 023131 (2020).
- [45] S. Sachdev, *Quantum Phase Transitions*, 2nd ed. (Cambridge University Press, 2011).
- [46] V. Rollano, M. C. de Ory, C. D. Buch, M. Rubín-Osanz, D. Zueco, C. Sánchez-Azqueta, A. Chiesa, D. Granados, S. Carretta, A. Gomez, S. Piligkos, and F. Luis, High cooperativity coupling to nuclear spins on a circuit quantum electrodynamics architecture, *Commun. Phys.* **5**, 10.1038/s42005-022-01017-8 (2022).
- [47] D. MacNeill, J. T. Hou, D. R. Klein, P. Zhang, P. Jarillo-Herrero, and L. Liu, Gigahertz frequency antiferromagnetic resonance and strong magnon-magnon coupling in the layered crystal CrCl_3 , *Phys. Rev. Lett.* **123**, 047204 (2019).
- [48] C. W. Zollitsch, S. Khan, V. T. T. Nam, I. A. Verzhbitskiy, D. Sagkovits, J. O’Sullivan, O. W. Kennedy, M. Strungaru, E. J. G. Santos, J. J. L. Morton, G. Eda, and H. Kurebayashi, Probing spin dynamics of ultra-thin van der waals magnets via photon-magnon coupling, *Nat. Commun.* **14**, 2619 (2023).
- [49] M. Mergenthaler, J. Liu, J. J. Le Roy, N. Ares, A. L. Thompson, L. Bogani, F. Luis, S. J. Blundell, T. Lancaster, A. Ardavan, G. A. D. Briggs, P. J. Leek, and E. A. Laird, Strong coupling of microwave photons to antiferromagnetic fluctuations in an organic magnet, *Phys. Rev. Lett.* **119**, 147701 (2017).
- [50] S. Martínez-Losa del Rincón, I. Gimeno, J. Pérez-Bailón, V. Rollano, F. Luis, D. Zueco, and M. J. Martínez-Pérez, Measuring the magnon-photon coupling in shaped ferromagnets: Tuning of the resonance frequency, *Phys. Rev. Appl.* **19**, 014002 (2023).
- [51] F. Queisser and R. Schützhold, Hierarchy of double-time correlations, *J. Stat. Mech.: Theory Exp* **2023**, 053101 (2023).
- [52] A. Gómez-León, Hierarchy of correlations: Application to green’s functions and interacting topological phases, *Phys. Rev. B* **94**, 035144 (2016).
- [53] A. Gómez-León, Hierarchy of correlations for the ising model in the majorana representation, *Phys. Rev. B* **96**, 064426 (2017).
- [54] B. Pérez-González, Álvaro Gómez-León, and G. Platero, Topology detection in cavity qed, *Phys. Chem. Chem. Phys.* **24**, 15860–15870 (2022).
- [55] O. Dmytruk and M. Schirò, Controlling topological phases of matter with quantum light, *Commun. Phys* **5**, 271 (2022).
- [56] B. Pérez-González, G. Platero, and Álvaro Gómez-León, Light-matter correlations in quantum floquet engineering (2023), [arXiv:2302.12290](https://arxiv.org/abs/2302.12290).
- [57] A. Gómez-León, Spin bath dynamics and dynamical renormalization group, *Phys. Rev. B* **100**, 094308 (2019).